

Nicole Steinmann, BSc

**Selective Ammonium and Ammonia Optical Sensors based on  
Crown Ether Receptors**

**MASTER'S THESIS**

to achieve the university degree of

Master of Science (MSc)

Master's degree programme: Technical Chemistry

submitted to

**Graz University of Technology**

Supervisor

Univ.-Prof. Dipl.-Chem. Dr.rer.nat. Ingo Klimant

Institute of Analytical Chemistry and Food Chemistry

Graz, October 2017



Toutes les grandes personnes ont d'abord été des enfants...  
mais peu d'entre elles s'en souviennent.  
*All grown-ups were once children...*  
*but only few of them remember it.*  
Antoine de Saint-Exupéry



---

## Abstract

This thesis describes a novel sensing mechanism for the optical detection of ammonia and ammonium based on fluoroionophores. The detection principle for both analytes is based on the complexation of an ammonium ion by a crown ether. This receptor is linked to a fluorescent indicator dye and fluorescence emission increases upon complexation of the ammonium ion.

Fluoroionophore based optical sensing relies on the principle of the photoinduced electron transfer (PET) effect, which is a redox reaction in the excited state of a fluoroionophore. This reaction is highly influenced by its environment. For this reason, the influence of the polarity of different solvents on the PET efficiency of the fluoroionophore was investigated. The PET effect is typically stronger in more polar solvents and is weakened in an apolar environment. The initial concept was an immobilization of the fluoroionophore in hydrophobic matrices, but due to the polarity of its environment it was not possible to obtain a suitable sensing material using the hydrophobic matrix. Therefore, hydrophilic matrices were tested.

To exclude ionic species (for example  $K^+$ ,  $Na^+$ ) the sensor was covered with an ion impermeable protective layer. Ammonia can still diffuse through it. An internal buffer system with a low pH value is used to protonate ammonia into ammonium ions, which are then detected. After optimizations, fast response and recovery times to ammonium were obtained, as well as good reversibility of the sensor. It has no hysteresis drift and is stable to pH changes. A great improvement over all existing sensors is, that this sensor showed no response to trimethylamine and dimethylamine, which is very important for environmental or biotechnological applications.

During this thesis, the synthesis of an optimized crown ether, and further on the fluoroionophore with this new receptor, was prepared. The idea was to increase the diameter of the cavity of the crown ether ([18]crown-6) by adding an additional  $CH_2$ -group to it. Thus, it should be more sensitive to ammonium ions.



---

## Kurzfassung

Ziel dieser Arbeit war, ein neuartiges Konzept für die optische Messung von Ammoniak und Ammonium-Ionen zu entwickeln. Das Nachweisprinzip beider Analyten beruht auf der Komplexbildung eines Ammonium-Ions in einem Kronenether, der als Rezeptor fungiert. Dieser Rezeptor ist mit einem Fluoreszenzindikatorfarbstoff gebunden, durch den bei einer Komplexbildung eine Fluoreszenzerhöhung stattfindet, welche aufgrund des PET (Photoinduced electron transfer) Effekts funktioniert.

Der PET-Effekt ist eine Redoxreaktion im angeregten Zustand eines Fluoroionophors, die stark von ihrer Umgebung beeinflusst wird. Aus diesem Grund wurde der Einfluss der Polarität verschiedener Lösungsmittel auf die PET-Effizienz der Fluoroionophore untersucht. Üblicherweise ist der PET-Effekt in polaren Lösungsmitteln ausgeprägter als in unpolaren. Die grundlegende Idee war, einen Farbstoff in einer hydrophoben Matrix zu immobilisieren und zu vermessen, jedoch war das aufgrund der im System gegebenen Polarität nicht möglich, deshalb wurden auch hydrophile Matrizen untersucht. Um Ionen (zum Beispiel  $K^+$ ,  $Na^+$ ) auszuschließen, wurde über die Sensorschicht noch ein Teflon Filter aufgelegt. Ammoniak kann durch diese Membran hindurch diffundieren und wird durch einen internen Puffer, mit niedrigem pH-Wert, zu Ammonium-Ionen protoniert, welche detektiert werden können. Nach der Entwicklung des besten Sensoraufbaus wurden schnelle Reaktions- und Wiederherstellungszeiten, sowie eine Reversibilität des Sensors erreicht. Des Weiteren wurde auch kein Hysterese Drift festgestellt und das System ist stabil gegenüber pH-Änderungen. Quersensitivitäten gegenüber Trimethylamin und Dimethylamin können aufgrund der Struktur des Kronenethers ausgeschlossen werden, was für Umwelt- oder biotechnologische Anwendungen sehr wichtig ist.

Teil dieser Arbeit war auch, den Kronenether ([18]Krone-6) zu optimieren. Dafür wurde eine zusätzliche  $CH_2$ -Gruppe in die Krone eingebaut um den Durchmesser zu vergrößern, um somit die Sensitivität auf Ammonium-Ionen erhöhen zu können.





---

## EIDESSTATTLICHE ERKLÄRUNG

Ich erkläre an Eides statt, dass ich die vorliegende Arbeit selbstständig verfasst, andere als die angegebenen Quellen/Hilfsmittel nicht benutzt, und die den benutzten Quellen wörtlich und inhaltlich entnommenen Stellen als solche kenntlich gemacht habe. Das in TUGRAZonline hochgeladene Textdokument ist mit der vorliegenden Masterarbeit identisch.

## AFFIDAVIT

I declare that I have authored this thesis independently, that I have not used other than the declared sources/resources, and that I have explicitly indicated all material which has been quoted either literally or by content from the sources used. The text document uploaded to TUGRAZonline is identical to the present master's thesis.

---

Datum/Date

---

Unterschrift/Signature



---

## Danksagung

An erster Stelle möchte ich mich bei Prof. Ingo Klimant bedanken, der es mir ermöglicht hat, die Zeit während meiner Masterarbeit auf diesem tollen Institut und mit den besten Arbeitskollegen verbringen zu dürfen. Danke dafür, und für die vielen Inputs und Ratschläge zu meiner Arbeit.

An dieser Stelle auch ein großes Dankeschön an Sergey, der immer zur Stelle ist, wenn etwas mal nicht klappt und gleich viele Vorschläge auf Lager hat, wie es denn funktionieren könnte.

Lieber Berni, du begleitest mich schon seit meinem ersten Semester hier in Graz. Du warst nicht nur der beste Ersti Tutor, sondern bist auch der allerbeste Betreuer den es gibt!! Danke für dein Vertrauen in mich und für deine Engelsgeduld mit meinen hunderttausend Baustellen auf einmal!

Natürlich darf die beste Arbeitsgruppe der Welt nicht fehlen! Danke für die vielen gemeinsamen Mittagessen, Wandertöpfe, sportlichen Aktivitäten und diversen Feierabend- und Dachterrassenge Getränke.

Liebe Dumpfbacken, ohne euch wäre mein Studium nur halb so schön gewesen! Danke für die vielen gemeinsamen Lern-, aber vor allem auch Feierstunden. Ich hoffe auf noch viele weitere Ouzo Umtrünke mitn Hucknbleibbär, zukünftige Serienabende und viele gemütliche Grillfeiern. Einen großen Dank an Anna dafür, dass du dir die Zeit genommen hast, meine Arbeit so gewissenhaft zu korrigieren.

Vielen Dank auch an Magdalena, Kerstin und Lena, die mir die Lernpausen mit tollen Klettertrips, Grillereien, Bauernscharade, Kaffeetratschen und Spritzer Abenden versüßt haben.

Liebe Jenni, ich bin froh, dass sich zwischen uns so eine tolle Freundschaft entwickelt hat, und hoffe, dass diese noch lange bestehen bleibt! Danke für deine unermüdliche Geduld mir zuzuhören und mir mit Rat und Tat zur Seite zu stehen.

---

Denjenigen, die mich nicht nur während meines Studium begleitet haben, sondern mich überhaupt erst ermutigt haben, es zu versuchen, gebührt natürlich ein ganz großes Dankeschön. Dazu gehören auf jeden Fall Kerstin, Hannes und Laro. Ich habe euch wirklich sehr ins Herz geschlossen und bin froh darüber, euch in meinem Leben zu haben. Steffi, du Ulknudl, du bist immer für jeden Spaß zu haben und das finde ich großartig.

Meine liebe Lisa, du haltest es schon am aller längsten mit mir aus und dafür möchte ich dir danken! Du hast immer ein offenes Ohr für mich und stärkst mir immer den Rücken, auch wenn wir manchmal nicht der gleichen Meinung sind. Du bist ein fixer Bestandteil meines Lebens und das wird für immer so bleiben.

Lieber Luki, Danke, dass du mich immer unterstützt, sei es um auf Reisen zu gehen, oder während dem Fertigwerden meines Studiums. Das letzte Jahr wäre ohne dich nur halb so schön gewesen. Ich hoffe auf noch viele weitere gemeinsame Abenteuer mit dir.

Zu guter Letzt, möchte ich noch meiner Familie danken, ohne die all das gar nicht möglich gewesen wäre. Danke, dass ihr mich immer in allem unterstützt habt und es mir leichtmacht, immer wieder gerne nach Hause zu kommen.

Mama und Papa, Danke, dass ihr es mir ermöglicht habt, ein so sorgenfreies Leben in Graz führen zu können. Ihr habt mich in all meinen Entscheidungen immer unterstützt, habt meine Spinnereien ausgehalten und wart trotzdem immer für mich da. Danke auch dafür, dass ihr die Reiselust in mir geweckt habt und sie mich auch ausleben habt lassen.

Nicole Steinmann, BSc

Graz, October 2017

---

# Contents

<b>1</b>	<b>Introduction</b>	<b>1</b>
<b>2</b>	<b>Theoretical Background</b>	<b>3</b>
2.1	Luminescence . . . . .	3
2.1.1	Absorption . . . . .	4
2.1.2	Transition between Electronic States . . . . .	5
2.1.3	Characteristics of Luminescence . . . . .	6
2.1.4	Quenching . . . . .	7
2.2	Fluorescence Sensors . . . . .	7
2.2.1	Fundamental Aspects . . . . .	7
2.3	Ion Sensors . . . . .	9
2.3.1	Ion Selective Electrode - ISE . . . . .	9
2.3.2	Ionophore Based Optical Sensors - IBOS . . . . .	10
2.3.3	Fluoroionophore Based Optical Sensors - FBOS . . . . .	11
2.3.4	Sensor Requirements for Cation Sensing . . . . .	13
2.4	Ammonia . . . . .	15
2.4.1	Ammonia Sources . . . . .	15
2.4.2	Application Areas of Ammonia . . . . .	16
2.4.3	Sensing Principles for Ammonia . . . . .	17
2.4.4	Optical Ammonia Sensors . . . . .	18
2.4.5	Novel Method for Ammonia Sensing . . . . .	19
<b>3</b>	<b>Materials and Methods</b>	<b>21</b>
3.1	Chemicals . . . . .	21
3.1.1	Plasticizers . . . . .	21
3.1.2	Polymers . . . . .	22
3.1.3	List of Chemicals . . . . .	23
3.1.4	List of Solvents . . . . .	24
3.2	Structural Measurements . . . . .	24
3.2.1	NMR - Nuclear Magnetic Resonance Spectroscopy . . . . .	24
3.2.2	GC-MS - Gas Chromatography - Mass Spectrometry . . . . .	24
3.3	Chromatography . . . . .	24
3.3.1	TLC - Thin Layer Chromatography . . . . .	24

3.3.2	Flash Column Chromatography . . . . .	25
3.4	Optical Characterization . . . . .	25
3.4.1	Absorption . . . . .	25
3.4.2	Emission and Excitation . . . . .	25
3.4.3	Interpretation of Spectra . . . . .	25
3.5	Sensor Film Measurement . . . . .	25
3.5.1	Buffer Preparation . . . . .	25
3.5.2	Sensor Foils . . . . .	26
3.5.3	Optical Measurement . . . . .	26
3.6	Chemical Treatment . . . . .	26
3.6.1	Hydrogenation . . . . .	26
<b>4</b>	<b>Experimental</b>	<b>27</b>
4.1	Sensor Preparation - Hydrophobic System . . . . .	27
4.1.1	Buffer Solutions . . . . .	27
4.1.2	Polymer/Plasticizer Cocktails . . . . .	27
4.1.3	Lipophilic Ammonium Salts . . . . .	28
4.2	Sensor Preparation - Hydrophilic System . . . . .	29
4.2.1	Polymer Studies - Composition of Cocktails . . . . .	29
4.2.2	Buffer Solutions . . . . .	29
4.2.3	Cocktail Preparation . . . . .	31
4.3	Synthesis . . . . .	32
4.3.1	1-(2-Methoxyethoxy)-2-nitrobenzene ( <b>1</b> ) . . . . .	32
4.3.2	2-(2-Methoxyethoxy)-aniline ( <b>2</b> ) . . . . .	32
4.3.3	(((2-Methoxyethoxy)phenyl)amino)-ethanol ( <b>3</b> ) . . . . .	33
4.3.4	3-((2-Hydroxyethyl)(2-(2-methoxyethoxy)phenyl)amino)propan-1-ol ( <b>4</b> ) . . . . .	34
4.3.5	Tetraethylene glycol ditosylate ( <b>5</b> ) . . . . .	34
4.3.6	NH <sub>4</sub> <sup>+</sup> Crown ( <b>6</b> ) . . . . .	35
4.3.7	NH <sub>4</sub> <sup>+</sup> Crown Aldehyde ( <b>7</b> ) . . . . .	36
<b>5</b>	<b>Results and Discussion</b>	<b>37</b>
5.1	Scope of this Thesis . . . . .	37
5.2	Part 1: Hydrophobic Matrices . . . . .	39
5.2.1	Influence of Solvent Polarity to the PET Efficiency . . . . .	39
5.2.2	Influence of Polymer Polarity on the PET Efficiency . . . . .	40
5.2.3	Plasticizer and Acid Concentration Screening . . . . .	41
5.2.4	Using Lipophilic Ammonium Salts . . . . .	43
5.3	Part 2: Hydrophilic Matrices . . . . .	45
5.3.1	Polymer Studies . . . . .	45
5.3.2	Influence of Internal Buffer . . . . .	47

---

5.3.3	Influence of Internal pH Value . . . . .	48
5.3.4	Hysteresis and Response Times . . . . .	49
5.3.5	Cross Sensitivity to different pH Values of the Sample . . . . .	50
5.3.6	Cross Sensitivity to other Amines and Potassium . . . . .	50
5.3.7	Further Investigations . . . . .	51
5.4	Part 3: Synthesis of Crown Ether and Fluoroionophore . . . . .	53
5.4.1	Synthesis Overview . . . . .	54
5.4.2	Crown Ether Synthesis . . . . .	55
5.4.3	Crown Aldehyde Synthesis . . . . .	55
5.4.4	Fluoroionophore Synthesis . . . . .	55
<b>6</b>	<b>Conclusion and Outlook</b>	<b>57</b>
<b>7</b>	<b>References</b>	<b>59</b>
<b>8</b>	<b>List of Figures</b>	<b>63</b>
<b>9</b>	<b>List of Tables</b>	<b>65</b>
<b>10</b>	<b>Appendix</b>	<b>67</b>
10.1	<sup>1</sup> H-NMR Spectra . . . . .	67
10.2	Abbreviations . . . . .	74





---

# 1 Introduction

Ammonia is a colorless gas with a strong pungent smell and it is toxic to humans and animals. Many processes on earth release ammonia and therefore, a detection for example in industry, medicine or the environment is of high interest.

Typical ammonia sensors are based on the deprotonation of a pH indicator dye caused by  $\text{NH}_3$ , which results in a change of the optical properties of the indicator dye. However, this system is not selective towards  $\text{NH}_3$  because other volatile bases can also deprotonate the pH indicator. In the work of West et al. an optical  $\text{NH}_3$  sensor, which is also based on a pH indicator dye, is presented. It was shown that an introduction of an ionophore for selective complexation of the generated ammonium ion can increase the selectivity of the sensor. [1]

In this work a fluoroionophore is used as indicator instead of a pH indicator. This is due to the fact that fluoroionophores respond directly and selectively to the ammonium ion which can be generated from ammonia inside a sensor membrane. Therefore, no cross sensitivity to substituted amines is expected. This is of high interest, for example, in fish farming industry, because trimethylamine is a degradation product of fish, therefore, it occurs in high concentrations. Currently available optical ammonia sensors can not distinguish between ammonia and trimethylamine.

For this thesis a potassium sensor, which shows a cross sensitivity to ammonium, was used. [2] It was converted into a highly selective  $\text{NH}_3$  sensor by covering the sensor membrane with a teflon layer. Such ion impermeable filters prevent a response of the sensor to ionic species, but  $\text{NH}_3$  can still diffuse through the barrier. An internal buffer system was used to generate  $\text{NH}_4^+$ -ions inside the sensor.

Additionally, an optimization of the fluoroionophore was performed to increase the binding stability towards ammonium ions leading to a higher sensitivity of the sensing material. Therefore, an additional  $\text{CH}_2$ -group was added to the crown ether to increase the cavity of the crown which should then be more suitable for the size of the ammonium ion.

This work presents the first ammonia sensor based on fluoroionophores and will be the basis for future research in this area.



---

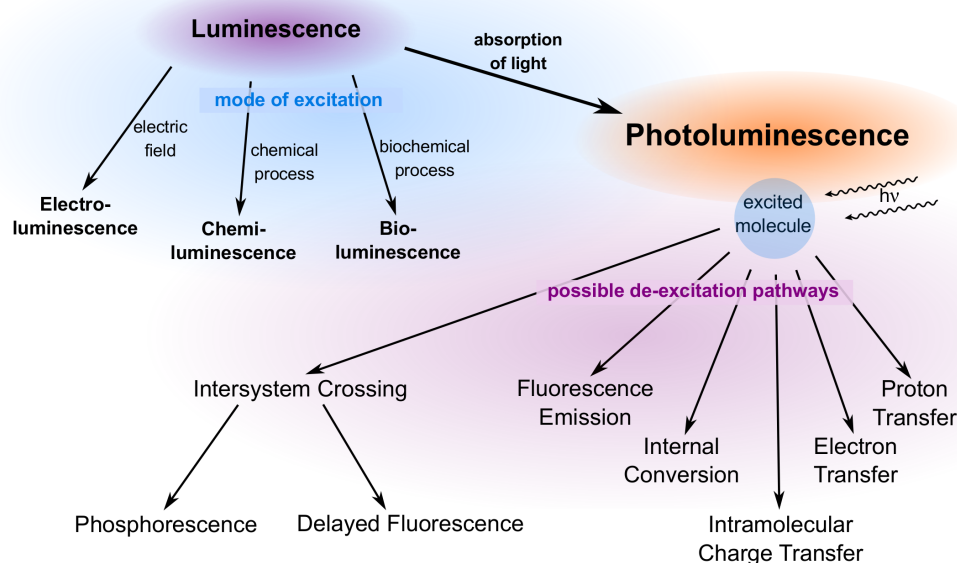
## 2 Theoretical Background

### 2.1 Luminescence

This chapter is based on references [3] and [4].

Luminescence is an emission of photons from an electronically excited species. These photons can have an energy ranging from ultraviolet to infrared light. Different kinds of luminescent compounds exist such as organic (aromatic hydrocarbons), inorganic (crystals, glasses) or organometallic compounds.

There are many types of luminescence which all differ in the mode of excitation as shown in figure 2.1. However, photoluminescence, which is caused by the absorption of light, will in particular be described in this thesis.



**Figure 2.1:**  
Luminescence - Overview:  
Different modes of excitation and possible de-excitation pathways.

### 2.1.1 Absorption

An electronic transition occurs if a photon is absorbed by a molecule, which takes the molecule in a so called excited state. Two types of orbitals are important in fluorescence spectroscopy: the highest occupied molecular orbital (HOMO) and the lowest unoccupied molecular orbital (LUMO). Both refer to the ground state of the molecule.

In equation 2.1 the electronic transitions are listed according to their energy difference.

$$n \rightarrow \pi^* < \pi \rightarrow \pi^* < n \rightarrow \sigma^* < \sigma \rightarrow \pi^* < \sigma \rightarrow \sigma^* \quad (2.1)$$

In fluorescence spectroscopy the main transitions are  $n \rightarrow \pi^*$  and  $\pi \rightarrow \pi^*$ . The energy of the  $\pi \rightarrow \pi^*$  transition decreases with an extended  $\pi$ -electron-system (conjugated linear or cyclic systems). This lower energy demand results in a larger wavelength of the absorption band.

### Beer-Lambert Law

The efficiency of light absorption at a certain wavelength is characterized by the absorbance and in most cases it follows the Beer-Lambert law which is shown in equation 2.2.

$$A = \log \frac{I^0}{I} = \epsilon * l * c \quad (2.2)$$

*A ... Absorbance [ $\lambda$ ]*

*I<sup>0</sup> ... Light intensity before entering the absorbing medium*

*I ... Light intensity after leaving the absorbing medium*

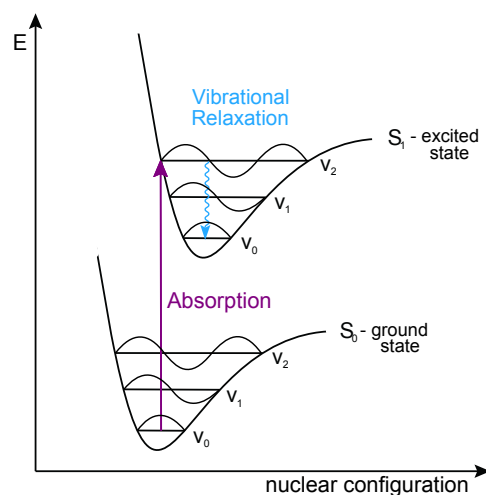
*$\epsilon$  ... Molar decadic absorption coefficient [ $L \text{ mol}^{-1} \text{ cm}^{-1}$ ]*

*l ... Absorption path length (length of cuvette) [cm]*

*c ... Concentration of the dye solution [ $\text{mol L}^{-1}$ ]*

### Franck-Condon Principle

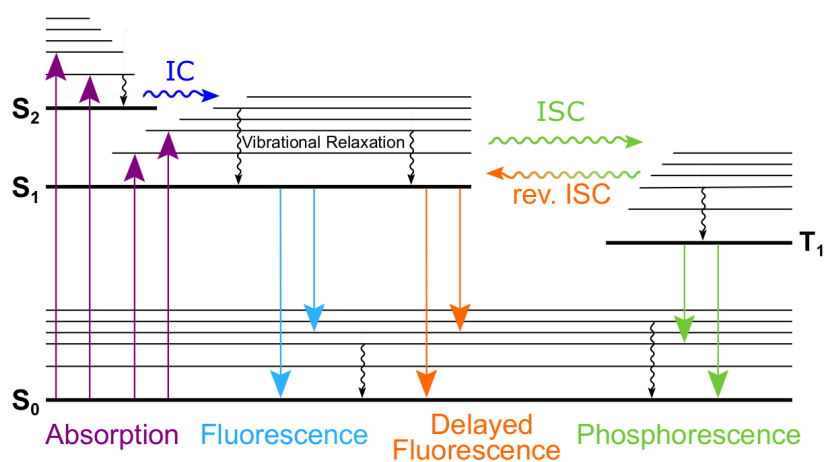
According to the Born-Oppenheimer approximation, the movement of electrons is much faster than the movement of the nuclei, therefore, the atoms can be considered as stationary. In figure 2.2 the vibronic transition is shown as a vertical arrow due to the assumption that the nuclear coordinates are constant during the transition.



**Figure 2.2:**  
Franck-Condon principle of a two-atom model

### 2.1.2 Transition between Electronic States

Many transitions between electronic states can happen before the molecule relaxes back to the ground state via emission of light. All processes that are occurring can be visualized in the Jablonski diagram which is shown in figure 2.3.



**Figure 2.3:**  
Jablonski Diagram:

Processes which occur between absorption and emission of light. In this figure  $S_0$  represents the ground state,  $S_1$  and  $S_2$  the excited singlet states and  $T_1$  the excited triplet state.

In figure 2.3  $S_0$  corresponds to the ground state. After absorption the electron is in a vibrational level of higher energy of the excited singlet state ( $S_1$ ). There are various subsequent transitions that can occur, which are discussed in the following sections.

### **Internal Conversion - IC**

Internal conversion is a non-radiative transition. It occurs between two electronic states with the same spin multiplicity. In figure 2.3 the internal conversion takes place from the level  $\mathbf{S}_2$  to  $\mathbf{S}_1$ .  $\mathbf{S}_1$  to  $\mathbf{S}_0$  is possible as well but it is less likely because of the large energy gap between these energy levels. Furthermore, this transition can compete with fluorescence and intersystem crossing and in the following with phosphorescence. The time scale for internal conversion is between  $10^{-13}$  and  $10^{-11}$  seconds.

### **Fluorescence**

Fluorescence occurs if the excited electron relaxes back to the ground state ( $\mathbf{S}_0$ ). This process happens during a time of around  $10^{-15}$  seconds. Due to the vibrational relaxation, emission is always occurring from the lowest vibrational level ( $\mathbf{S}_1$ ), which can clearly be seen in figure 2.3. For this reason, fluorescence spectra can be referred to as the "mirror spectrum" of absorption.

### **Intersystem Crossing - ISC**

Intersystem crossing is a transition from the singlet state ( $\mathbf{S}_1$ ) to the triplet state ( $\mathbf{T}_1$ ), which means that the electron changes its spin. This process is possible through spin-orbit coupling. The electron is then brought to the lowest vibrational level ( $\mathbf{T}_1$ ) and from there **Phosphorescence** is occurring. The lifetime of the triplet state is usually in the range of milliseconds to seconds, but the time of the emission of photons equals the time of the emission in fluorescence ( $10^{-15}$  s).

There is another possibility for the electron besides phosphorescence. If the energy difference is small enough and the lifetime of the triplet state is sufficiently long, **reverse Intersystem Crossing** can occur, which results in an emission with the same spectrum as in normal fluorescence, but with much longer lifetimes. This transition is called **Delayed Fluorescence**.

## **2.1.3 Characteristics of Luminescence**

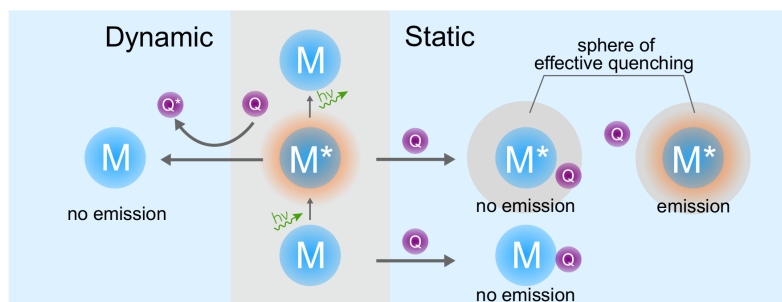
**Lifetime** and **Quantum Yield** are two important terms in respect to the characterization of luminescence.

Lifetime measurements give the time which is needed for 63% of the excited electrons to relax to the ground state.

The quantum yield is the ratio between the number of emitted and absorbed photons. Because of non-radiative de-excitation not all absorbed photons are emitted via fluorescence or phosphorescence.

### 2.1.4 Quenching

Quenching occurs if an excited molecule interacts with another molecule or with itself resulting in a de-excitation of the molecule. This means, the fluorescence intensity is decreasing. There are several processes that can cause such a de-excitation, for example, electron or proton transfer, energy transfer or the formation of excimers. There are two ways for this process, one is dynamic quenching and the other one static quenching. Figure 2.4 shows these two pathways.



**Figure 2.4:**  
Dynamic and Static Quenching  
M...molecule, M\*...excited molecule, Q...quencher

In **dynamic quenching**, both the luminescence lifetime and intensity are decreased upon interaction with the quencher.

**Static quenching** is observed if a complex between the molecule and the quencher is formed which is non-fluorescent. This process can happen either in the ground state of the molecule or in the excited state via a sphere of effective quenching. In the latter case the quencher has to be in the active sphere of the molecule, otherwise it has no effect on the excited molecule. In this case, the luminescence lifetime remains unchanged whereas the intensity is decreased.

## 2.2 Fluorescence Sensors

This chapter is based on reference [3].

### 2.2.1 Fundamental Aspects

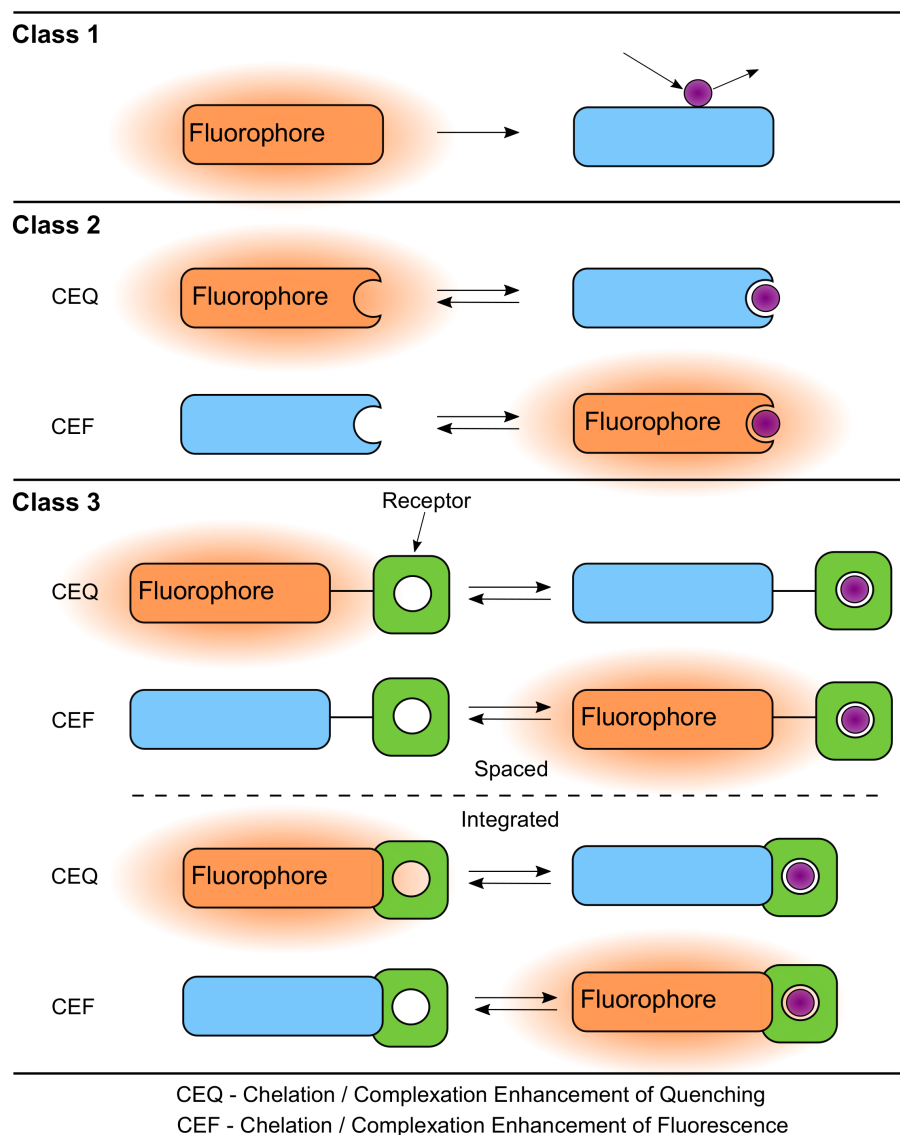
The design of fluorescence sensors is from high importance because of their wide application area for example in analytical chemistry, biochemistry, medicine or the environment.

Many analytes can be detected via fluorescence methods for example:

- cations:  $\text{Na}^+$ ,  $\text{K}^+$ ,  $\text{Ca}^{2+}$ ,  $\text{Mg}^{2+}$ ,  $\text{NH}_4^+$
- anions: halide ions, citrates, carboxylates
- neutral molecules: sugars (glucose)
- gases:  $\text{O}_2$ ,  $\text{CO}_2$

Fluorescence detection offers many advantages such as an increase of sensitivity, selectivity, local observation and response time compared to other methods such as absorption measurements. In fluorescent sensors, the fluorophore is the signaling species and acts as a transducer. A transducer converts the information if the receptor reacts or interacts in the presence of an analyte into an optical (or electrical for electrochemical sensors) signal.

Fluorescence sensors can be separated into three major classes which are shown in figure 2.5.



**Figure 2.5:**

Main classes of fluorescent sensors:

- class 1: no association - quenching by collision with an analyte
- class 2: complexing fluorophore
- class 3: fluorophore linked to a receptor (spaced or integrated)



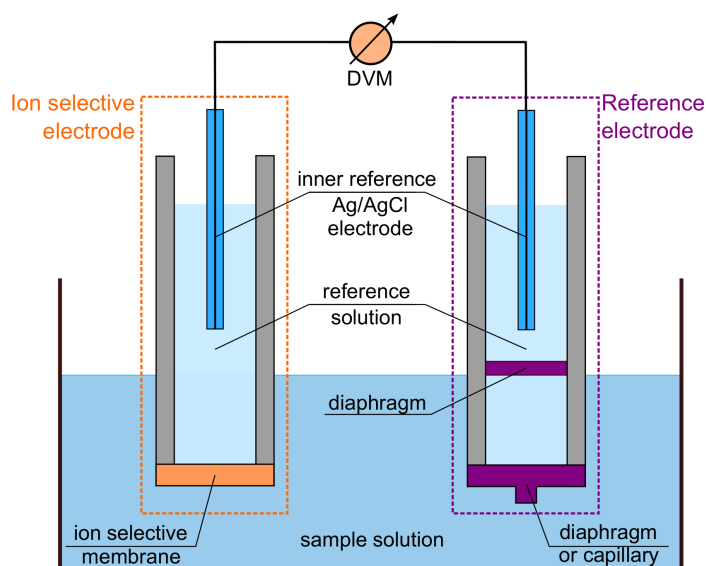
As illustrated in figure 2.5 there are three major classes of fluorescence sensors. In class 1 the fluorophore undergoes dynamic quenching upon a collision with an analyte. This method is already successfully applied for the measurement of dissolved  $O_2$  or even charged species such as chloride ions. The fluorophores from class 2 can reversibly bind an analyte. If the analyte is a proton, it is called a fluorescent pH indicator and if it is an ion it is called a fluorescent chelating agent. The fluorescence can either be increased (CEF: Chelation / Complexation Enhancement of Fluorescence) or quenched because of binding (CEQ: Chelation / Complexation Enhancement of Quenching). Class 3 sensors require an additional structural element which can be referred to as receptor and is responsible for the recognition of the analyte of interest, but is not involved in the signal transduction. Molecules, which are capable of sensing ionic species take advantage of an ionophore receptor coupled to a fluorophore. It is then referred to as fluoroionophore.

## 2.3 Ion Sensors

This chapter is based on references [5] and [6]. Other references will be cited independently.

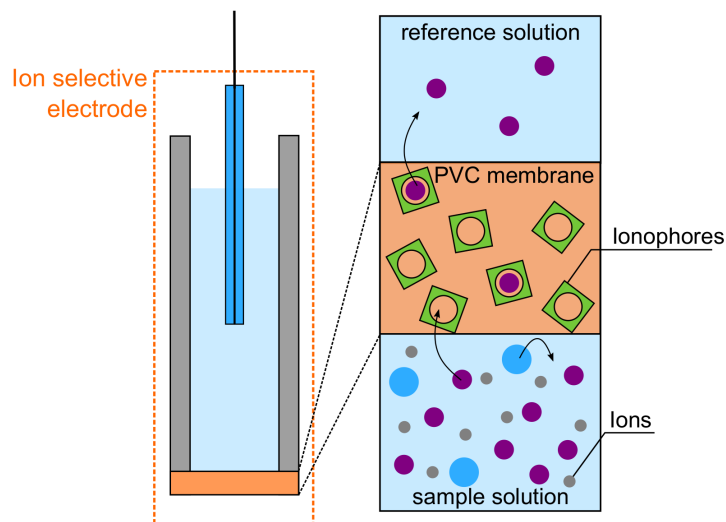
### 2.3.1 Ion Selective Electrode - ISE

An electrochemical cell consists of two so called half-cells. Such half-cells are an electrode-electrolyte combination. One cell is called ion selective cell and the other one is the reference cell. They are connected by a potential measuring device (digital voltmeter - DVM). The composition of the setup is illustrated in figure 2.6. [7]



**Figure 2.6:**  
Principal setup of an ISE

An ISE works with the potential difference that is measured between the reference cell and the ion selective cell. The measured potential is generated by the ions which are selected across an ion selective membrane (figure 2.7) in comparison to the reference electrode. This potential is the net potential and is directly proportional to the activity of the selected ion. This relationship can be described by the Nernst equation.



**Figure 2.7:**  
Representative working principle of an ion selective membrane,  
which is based on a liquid-solid membrane.

Different types of ISE exist for example:

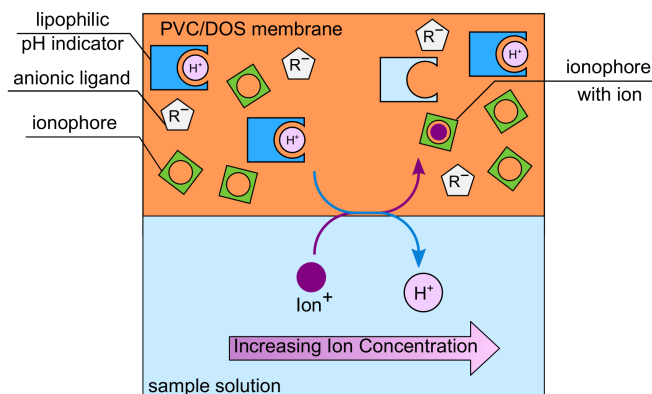
- solid state electrode (for anion sensing)
- glass membrane electrode (for monovalent cation sensing)
- liquid membrane electrode (for polyvalent cation sensing)

The liquid membrane electrode is the most common one for ion selective sensing. In general ISE are less expensive compared to other analytical techniques and they are simple to use. However, they still suffer from several drawbacks such as the tendency to drift due to the reference electrode. Additionally, miniaturization cannot be easily performed due to bulky electrodes. Optical sensors can overcome this limitations and will be described in more detail in the following section.

### 2.3.2 Ionophore Based Optical Sensors - IBOS

The principle of IBOS is indirect sensing, which means that the binding of an analyte to a receptor causes a secondary, optically detectable process. [8]

The sensor membrane typically consists of a polymer matrix (PVC) with additional plasticizer (DOS) to increase the ion mobility within the membrane. Incorporation of ionophores, lipophilic pH indicators and anionic ligands result in an IBOS. Such a membrane is shown in figure 2.8.



**Figure 2.8:**  
Scheme of the ion-exchange process [8]

The ionophores have a high affinity towards the desired cations and due to this property the cations are drawn into the membrane and an equivalent amount of protons from the lipophilic pH indicator is released out of the membrane. The change in the protonation degree of the lipophilic pH indicator leads to an optical signal which can be detected. The disadvantage of such sensor systems is their pH cross-sensitivity. A simultaneous measurement of the pH value could be done to overcome this, but it results in a more complex system.

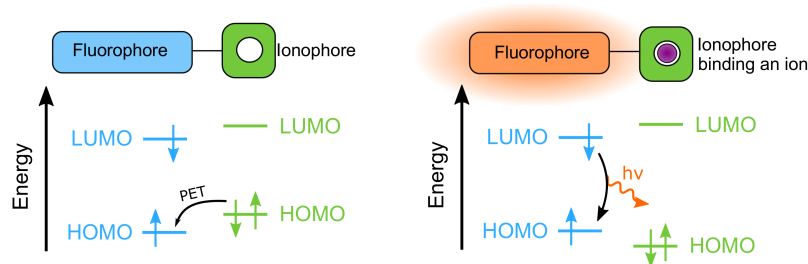
### 2.3.3 Fluoroionophore Based Optical Sensors - FBOS

FBOS are one of the few strategies which are used to overcome the pH dependency of an IBOS. A fluoroionophore is a combination of the fluorophore (transducer) and the ionophore (receptor) as described in chapter 2.2.1.

The principle of FBOS is based on fluorescence quenching, which can occur either via a photoinduced electron transfer (PET) or via an intramolecular charge transfer (ICT). [9]

#### Photoinduced Electron Transfer - PET

The PET effect occurs, if an excited electron is transferred from an electron donor to an acceptor. To observe a PET effect it is important that the HOMO of the ionophore (donor) is energetically higher than the HOMO of the fluorophore (acceptor), which is shown in figure 2.9. If an ion is bonded to the ionophore the energetic level of the HOMO is reduced. Due to this reduction the transfer of the electron is not possible anymore and there is no PET effect. This results in an increase of fluorescence. [10]

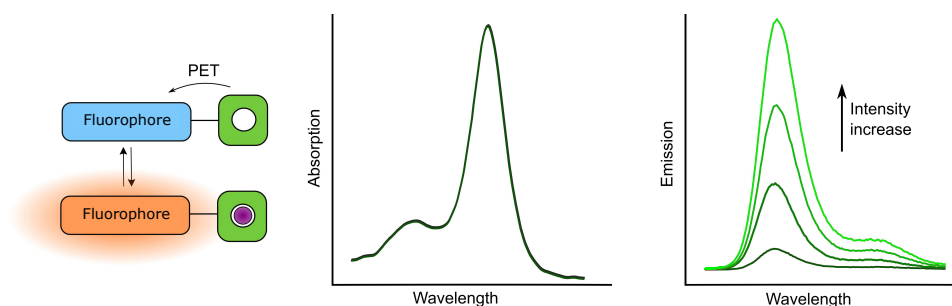
**Figure 2.9:**

PET effect from the molecular orbital point of view

left picture - PET effect is observed due to the higher HOMO level of the ionophore

right picture - no PET effect due to the binding of an ion to the ionophore

The PET effect causes only differences in the luminescence intensity of the fluorescence, which means that the fluorescence increases with a higher ion concentration but the emission spectra stay the same as shown in figure 2.10.

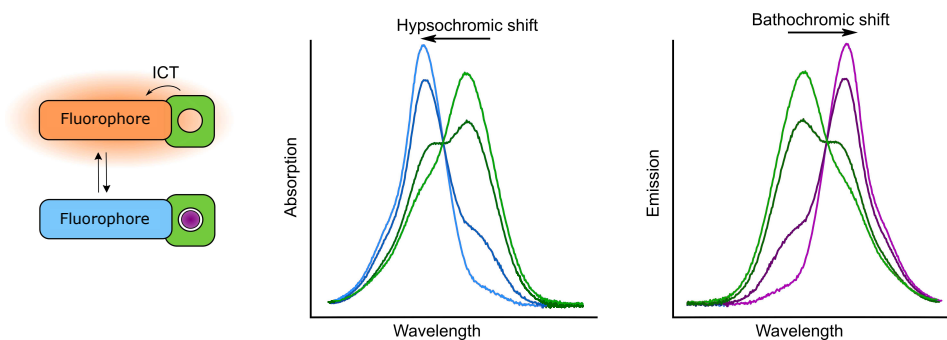
**Figure 2.10:**

Schematic presentation of a PET based sensor:

Fluorescence increase is obtained with higher analyte concentration, due to a reduction of the PET effect.

### Intramolecular Charge Transfer - ICT

In contrast to the PET effect, the ICT effect causes a change in the photophysical properties, which results in a hypsochromic or bathochromic shift of the absorption band depending on the chosen ionophore (shown in figure 2.11). [9] As this indicator shows luminescence too, when the analyte is absent, it is possible to perform for example ratiometric measurements.

**Figure 2.11:**

ICT effect:

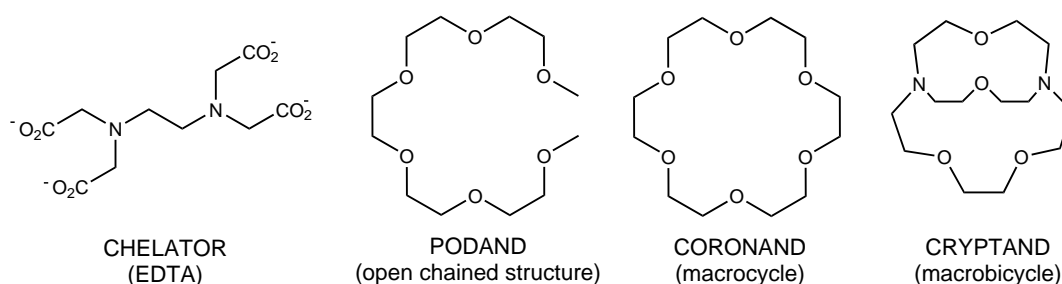
Ionophore as donor - hypsochromic (blue) shift  
 Ionophore as acceptor – bathochromic (red) shift

### 2.3.4 Sensor Requirements for Cation Sensing

The characteristics of the ionophore and the expected changes in fluorescence of the fluorophore are very important. For example, the stability of a receptor-cation-complex depends on many factors such as:

- nature of the solvent
- nature of the cation
- temperature
- ionic strength
- and the pH value.

For ion sensing the selectivity is of high importance, which means that the complexation of a certain cation is possible even in the surrounding of other cationic species. Therefore, the ionophore should match the characteristics of the cation, for example, in ionic diameter, coordination number or charge density. There are several types of molecules which can act as an ionophore. They are shown in figure 2.12.

**Figure 2.12:**

Examples of ionophores

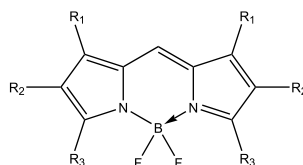
## Crown Ether Ionophores

Different sizes of crown ethers are very good to bind ions ( $\text{Na}^+$ ,  $\text{K}^+$  or  $\text{NH}_4^+$ ). Depending on the radius of the desired cation a proper crown ether is used as ionophore. Ions which fit in the cavity of the crown can easily be measured. [11] However, some ions cannot be distinguished just by size. An example is the determination of  $\text{K}^+$  and  $\text{NH}_4^+$  as the size of the ions is similar. Therefore, they are each other's interferent.

## BODIPY Fluorophores

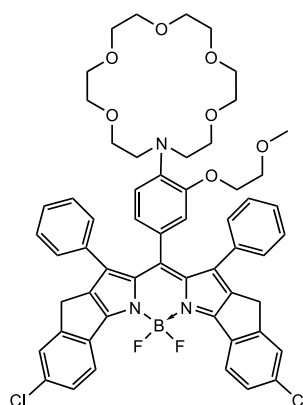
Another important factor in the development of new fluoroionophores, besides a suitable receptor unit, is the used fluorophore. The highly fluorescent borondipyrromethene (BODIPY) dye was first discovered by Treibs and Kreuzer. [12] Such dyes have many advantages, for example:

- high quantum yields
- sharp absorbance and emission bands
- high stability in physiological pH-range
- decomposition only under strong acidic/basic conditions. [13]



**Figure 2.13:**  
Basic structure of a BODIPY fluorophore

The aim of this thesis was to produce a selective ammonium/ammonia sensor. This sensor is based on a crown ether as ionophore and a BODIPY with suitable residues as fluorophore. In figure 2.14 an already existing fluoroionophore is shown. [2] This compound was used in the search of a new sensor setup.



**Figure 2.14:**  
Fluoroionophore

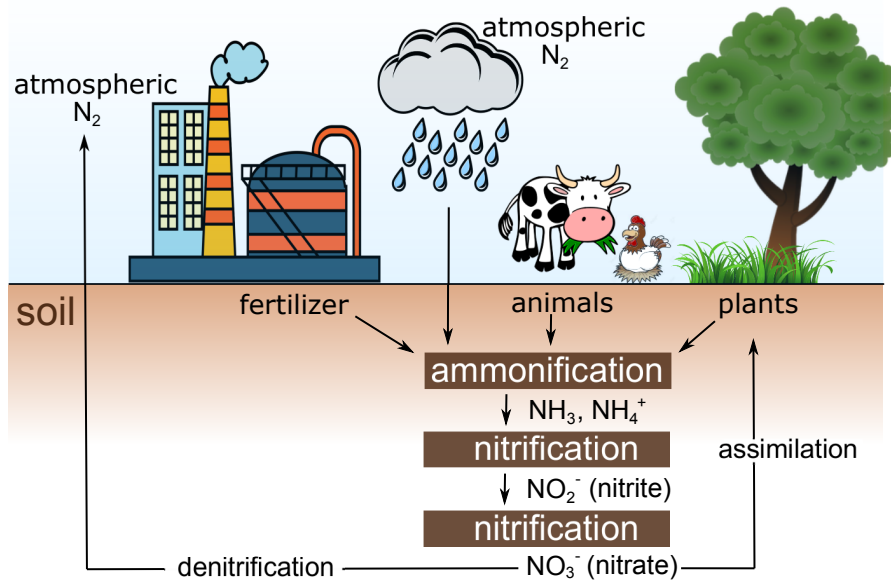
## 2.4 Ammonia

This chapter is based on reference [14]. Other references will be cited independently.

Ammonia is a colorless gas with a strong pungent smell and it is toxic to humans and animals. Therefore, detection of ammonia is of high interest. The following chapters will give a short overview about ammonia sources, application areas for ammonia sensors and ammonia sensing principles.

### 2.4.1 Ammonia Sources

Most of the ammonia which is in our atmosphere is emitted either directly or indirectly by human activity. In 2005 the worldwide emission of ammonia per year was around 48 teragram. [15] In this thesis the three major classes of ammonia sources are described. A summary of these processes is given by the nitrogen cycle which is shown in figure 2.15.



**Figure 2.15:**  
Schematic representation of the nitrogen cycle.

### Ammonification

Ammonification takes place if animal, plant and microbial biomass is recycled after its death. A series of metabolic activities decompose organic nitrogen. This process is performed by microorganisms, which release ammonia or ammonium ions.

## **Nitrification**

Through the nitrification process atmospheric nitrogen can enter the ecosystem. Together with the residues from the ammonification it is converted to nitrate via two consecutive pathways. In the first part ammonia or ammonium is biological oxidized to nitrite and in the second part the nitrite is further oxidized to nitrate. [16]

## **Combustion**

For refrigeration systems and for the production of fertilizers ammonia is produced by the chemical industry via the Haber-Bosch process.

### **2.4.2 Application Areas of Ammonia**

Many processes on earth release ammonia (as shown in the nitrogen cycle). Therefore, a detection of ammonia, for example, in industry, medicine or the environment is of high interest. A high concentration is easy to detect, due to the strong pungent smell of the gas but for low concentrations, the human nose fails.

#### **Automotive Industry**

Air quality control in the passenger cabinet is one reason, why ammonia measurement is very important for this industry. This kind of measurement could be used to stop the air supply from outside if the ammonia concentration is higher due to a fire or nearby stables. Another example is the  $\text{NO}_x$  reduction in diesel engines or the monitoring of exhaust gases, as they form the main part of gaseous pollution. [17] 20 mg/s or up to 8 ppm ammonia have been measured in exhaust gases. [18]

#### **Environment**

Near farming areas or stables and if manure is distributed on fields the ammonia concentration in the air increases. If the concentration gets too high it is harmful to people and animals living nearby. Therefore, detection of ammonia is essential. The ammonia content in the natural atmosphere can differ, dependig on the location. In the Netherlands, for example, the average ammonia concentration is about 1.9 ppb. Near farming areas the concentration rises up to over 10 ppm. [19] Another application is a measurement of ammonia in the fish farming industry. It is of high interest because ammonia is a main metabolic waste product from fish. It is excreted through the urine and the gills.



## Chemical Industry

The Haber-Bosch process is the main method in chemical industry to produce ammonia. In the past the ammonia production was of high interest, because an inexpensive supply of nitrogen was needed for the production of nitric acid, which is a key component of explosives. Nowadays, the main part of the ammonia production is used for fertilizers, chemical production or refrigeration systems. The basic principle for such refrigeration systems is a closed cycle, where evaporation, compression, condensation and expansion happen. [20] As the chemical industry makes use of almost pure ammonia, an alarm system detection, which warns if the maximum allowed workspace ammonia concentration of 20 ppm is reached, is required.

## Medicine

Medicinal applications for ammonia sensing are for example the measurement of ammonia levels in exhaled air. This is of high interest for the diagnosis of certain diseases. The detection range for breath analysis is between 50 and 2000 ppm. [21] Another application is, to measure the ammonia concentration in blood, especially in sports medicine. [22]

### 2.4.3 Sensing Principles for Ammonia

For the measurement of ammonia many principles are known. The most common ones will be described in this section.

#### Metal-Oxide Gas Sensors

Metal-oxide gas sensors are mostly based on  $\text{SnO}_2$ . The underlying principle of such sensors is the conductance change, due to the chemisorption of the gas molecules to the sensing layer. The drawback is that they are not selective to one specific gas. [23] There are different approaches to overcome this drawback. Commercial available sensors are  $\text{WO}_3$  ammonia sensors with Au and  $\text{MoO}_3$  additives. They are used in combustion gas detectors or in gas alarm systems for example to detect an ammonia leakage in refrigeration systems. [24] The detection range of such sensors is from 1 to 1000 ppm. [25]

#### Catalytic Ammonia Sensors

Chemical cells can be used for detection of ammonia. Such cells work via a catalytic reaction of a metal layer with the gas in combination with a solid state ion conducting material as described earlier in section 2.3.1. The selectivity of such sensors depends on many factors, for example, the metal. Sensors based on palladium can reach a detection limit of 1 ppm. [26]

## **Conducting Polymer Gas Detectors**

Polymers can be used for ammonia detection as well. The oxidized form of, for example, polypyrrole [27] or polyaniline [28] can be reduced by ammonia. In this two-step process, ammonia reacts irreversibly with the polymer and then reversibly reduces the oxidized polymer. This reduction causes a conductivity change in the polymer film which can be detected amperometrically. The lower detection limit with polyaniline as conducting polymer is 1 ppm. [28] Due to the first irreversible reaction a mass increase in the polymer film occurs, which results in a decrease of the sensitivity over time.

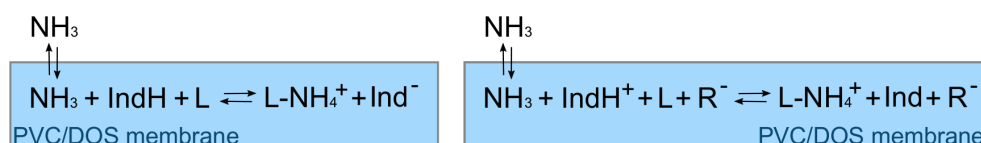
## **Optical Gas Analyzers**

There are two ways for optical ammonia detection, the first possibility is a **spectrophotometric detection**, which is about coloration of the analyte. This kind of analysis is used to detect the ammonia concentration in water. Well known is the Nessler reaction with dipotassium tetraiodomercurate(II) in a dilute alkaline solution as reagent. The big disadvantage is that the mentioned reagent is toxic. Another coloration method is the Berthelot reaction, where a blue coloration is obtained, due to a combination of ammonia, phenol and hypochlorite. [29] The detection limit is about 90 ppb. The drawbacks of these methods are the slow kinetics of the reactions.

The second possibility is an **optical absorption ammonia detection**. In such systems a light source is needed. The light passes an ammonium sensitive layer and the spectrum of the light, which reaches the detector is influenced through the material properties as a function of the gas composition. The general properties of the ammonium sensitive layer and the working principle will be described in the next section (2.4.4).

### **2.4.4 Optical Ammonia Sensors**

State of the art optical ammonia sensors are based on the principle of deprotonation of a pH indicator dye caused by ammonia. [1] This principle is described in section 2.3.2 (Ionophore Based Optical Sensors). The pH indicator is immobilized in a PVC/DOS membrane. The response to ammonium is based on two similar mechanisms, depending upon an acidic or basic pH indicator as shown in figure 2.16.

**Figure 2.16:**

Mechanism of acidic/basic pH indicator

left: reaction with an acidic indicator

right: reaction with a basic indicator - an additional anion is required

Ammonia diffuses into the PVC/DOS membrane and reacts with the components inside. The left part of the picture illustrates a reaction with an acidic indicator (IndH) and an ionophore (L), the right part of the picture shows the reaction with a basic indicator, an ionophore and a lipophilic anion ( $\text{R}^-$ ). The anion is necessary for keeping the electroneutrality inside the sensor. The ionophore selectively binds and stabilizes the ammonium ion and through this property the sensor system is more sensitive to ammonia. Without the ionophore other volatile bases are able to diffuse into the sensing layer as well, where they can cause the deprotonation of the dye. Therefore, they show a lower selectivity towards ammonia.

### 2.4.5 Novel Method for Ammonia Sensing

In this thesis a new concept for ammonia sensing will be shown. The concept relies on the principal of fluoroionophore based optical sensors, which are described in section 2.3.3.

To overcome the pH dependency of the sensor system a fluoroionophore indicator instead of a pH indicator is used. This is due to the fact that they respond directly and selectively to the ammonium ion. Therefore, no cross sensitivity to substituted amines is expected. This is of high interest, for example, in fish farming industry, because trimethylamine is a degradation product of fish, therefore, it occurs in high concentrations. Currently available optical ammonia sensors can not distinguish between ammonia and trimethylamine.

All further investigations are discussed in detail in chapter 5 (Results and Discussion).



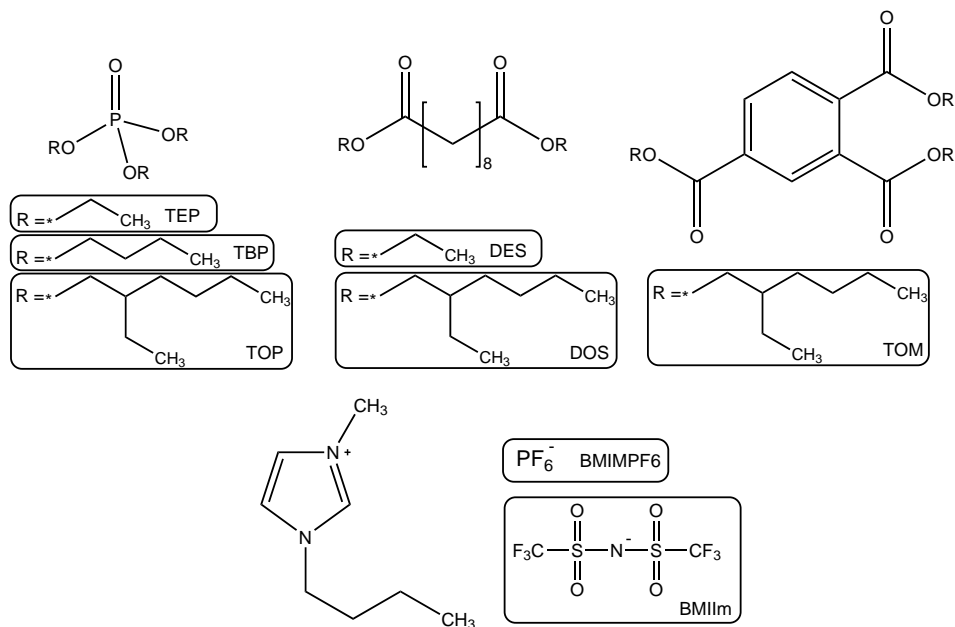
# 3 Materials and Methods

## 3.1 Chemicals

### 3.1.1 Plasticizers

**Table 3.1:** List of Plasticizers

Plasticizer	Abbreviation	Supplier	CAS-Number
1-Butyl-3-methylimidazolium-bis(trifluoromethylsulfonyl)imide	BMIIIm	Sigma-Aldrich	174899-83-3
1-Butyl-3-methylimidazolium-hexafluorophosphate	BMIMPF6	Sigma-Aldrich	174501-64-5
Diethyl sebacate	DES	TCI	110-40-7
Dioctyl sebacate	DOS	Fluka	122-62-3
Tributyl phosphate	TBP	Ehrenstorfer	126-73-8
Triethyl phosphate	TEP	TCI	78-40-0
Trioctyl phosphate	TOP	Sigma-Aldrich	78-42-2
Trioctyl trimellitate	TOM	TCI	3319-31-1

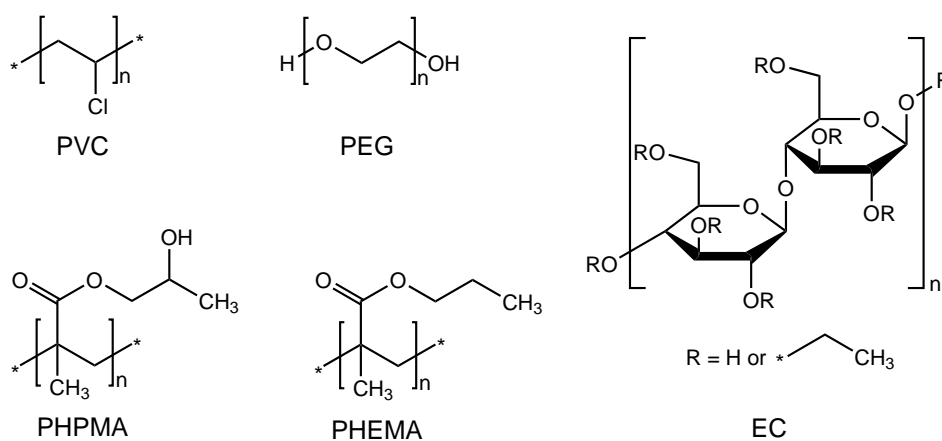


**Figure 3.1:**  
Plasticizer and ionic liquid structures

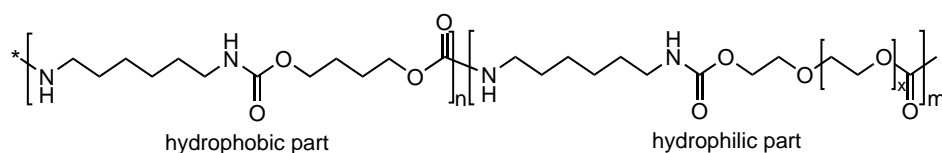
## 3.1.2 Polymers

Table 3.2: List of Polymers

Polymer	Abbreviation	Supplier	CAS-Number
Polyvinyl chloride	PVC	Fluka	9002-86-2
Ethyl cellulose	EC	Fluka	9004-57-3
Hydrogel D1	D1	AdvanSource biomaterials	
Hydrogel D4	D4	AdvanSource biomaterials	
Polyethylen glycol 3400	PEG 3400	Scientific Polymer Pr	35322-68
Polyethylen glycol 1000	PEG 1000	Sigma-Aldrich	25322-68-3
Polyhydroxyethyl methacrylate	PHEMA	Polyscience	25249-16-5
Polyhydroxypropyl methacrylate	PHPMA	Sigma-Aldrich	25703-79-1



**Figure 3.2:**  
Polymer structures



**Figure 3.3:**  
Possible hydrogel structure

## 3.1.3 List of Chemicals

Table 3.3: List of Chemicals

Chemicals	Abbreviation	Supplier	CAS-Number
2,3-Dichloro-5,6-dicyano-1,4-benzoquinone	DDQ	Sigma-Aldrich	84-58-2
2-[Bis(2-hydroxyethyl)amino]-2-(hydroxymethyl)propane-1,3-diol	BIS TRIS	Roth	6979-37-0
2-Amino-2-(hydroxymethyl)propane-1,3-diol	TRIS	Roth	77-86-1
2-Chloroethylmethylether		TCI	627-42-9
2-Nitrophenol		Sigma-Aldrich	88-75-5
3-(Cyclohexylamino)-1-propanesulfonic acid	CAPS	Roth	1135-40-6
Ammonium chloride		Sigma-Aldrich	12125-02-9
Boron trifluoride diethyl etherate		Sigma-Aldrich	09-63-7
Bromopropanol		TCI	627-18-9
Calcium carbonate		Merck	471-34-1
Chloroethanol		Sigma-Aldrich	107-07-3
Citric acid monohydrate		Merck	5949-29-1
Dinitrophenylhydrazine		Sigma-Aldrich	119-26-6
Hydrochloric acid		VWR	7647-01-0
Methylamine hydrochloride	MA	Acros	12125-02-9
N,N-Diisopropylethylamine	DIPEA	Sigma-Aldrich	7078-68-5
Ninhydrin		Fluka	485-47-2
Palladium hydroxide on carbon		Sigma-Aldrich	12135-22-7
Phosphoric acid		Merck	7664-38-2
Phosphoroxo chloride		Sigma-Aldrich	10025-87-3
Potassium carbonate		Sigma-Aldrich	584-08-7
Potassium hydroxide		Merck	1310-58-3
Potassium iodide		Roth	7681-11-0
p-Toluenesulfonyl chloride		TCI	98-59-9
Silica gel		Acros	112926-00-8
Sodium dihydrogen phosphate		Roth	7558-80-7
Sodium hydride		TCI	7646-69-7
Sodium chloride		Merck	7647-14-5
Sodium hydroxide		Merck	1310-73-2
Sodium sulfate		Roth	7757-82-6
Tetraethylene glycol		Sigma-Aldrich	112-60-7
Trifluoroacetic acid	TFA	Fluka	76-05-1
Trimethylamine hydrochloride	TMA	Acros	593-81-7

### 3.1.4 List of Solvents

**Table 3.4:** List of Solvens

<b>Solvent</b>	<b>Abbreviation</b>	<b>Supplier</b>	<b>CAS-Number</b>
Acetone		Brenntag	67-64-1
Cyclohexane	C	VWR	1100-82-7
Dichloromethane	DCM	Fisher Scientific	75-09-2
Dimethyl sulfoxide	DMSO	Roth	67-68-5
Dimethylformamide	DMF	Merck	68-12-2
Ethanol	EtOH	Brenntag	64-17-5
Ethyl acetate	EA	VWR	141-78-6
Methanol	MeOH	Roth	67-56-1
Tetrahydrofuran	THF	VWR	109-99-10
Toluene		Roth	108-88-3

## 3.2 Structural Measurements

### 3.2.1 NMR - Nuclear Magnetic Resonance Spectroscopy

The  $^1\text{H}$ -NMR spectra were recorded on a 300 MHz Bruker AVANCE III instrument. The obtained data were analyzed with MestReNova NMR software.

### 3.2.2 GC-MS - Gas Chromatography - Mass Spectrometry

The gas chromatography was performed via an Agilent Technologies 7890A GC-system with a polar Agilent Technologies J&W HP-5MS capillary column (30 m x 0.25 mm, 0.25  $\mu\text{m}$  film, (5 %-phenyl)-methylpolysiloxane) with He 5.0 as carrier gas in split mode. An Agilent Technologies 7683B series auto sampler injector was used. Before and after each injection the needle was rinsed with methanol and ethyl acetate. Electron impact (EI,  $E = 70\text{ eV}$ ) was used for ionization with the mass analyzer 5975C inert MSD with Triple-Axis Detector.

Temperature program: MT\_50\_S: 50  $^{\circ}\text{C}$  for 1 min, ramp 40  $^{\circ}\text{C}/\text{min}$  linear until 300  $^{\circ}\text{C}$ , then 300  $^{\circ}\text{C}$  for 5 min.

## 3.3 Chromatography

### 3.3.1 TLC - Thin Layer Chromatography

Silica gel plates from Merck (silica gel 60 F<sub>254</sub> aluminium sheets 20x20 cm) were used for the thin layer chromatography. They were detected via UV-light (254 nm and 366 nm) as well as with a suitable staining solution such as cer ammonium molybdate, dinitrophenylhydrazine, ninhydrine or  $\text{KMnO}_4/\text{H}_2\text{SO}_4$ . The plates were developed by a hot air stream.



### 3.3.2 Flash Column Chromatography

Silica gel from Acros Organics (0.035-0.070 mm, 60 Å, nitrogen flushed) was used for the purification of crude products.

## 3.4 Optical Characterization

### 3.4.1 Absorption

Absorption spectra were recorded on a VARIAN CARY 50 Conc, UV-Vis spectro-photometer. The measurements were carried out between 800 and 350 nm by using a fast scan rate with a baseline correction of the corresponding solvent. Hellma Analytics 100-OS 10 mm precision cuvettes were used.

### 3.4.2 Emission and Excitation

Emission and excitation spectra were obtained via a FluoroLog®3 spectrofluorometer from Horiba Scientific equipped with a R2658 photomultiplier from Hamamazu. Hellma Analytics 100-OS 10 mm precision cuvettes were used for the measurements.

### 3.4.3 Interpretation of Spectra

The spectra are normalized to the maximum of the baseline ( $F_0$ ). The obtained values ( $F/F_0$ ) are then plotted against the wavelength to obtain the normalized emission spectra.

For calibration spectra the maximum values (at a wavelength of 655 nm) were taken and plotted against the concentration.

For the kinetic spectra the sensor was excited at 635 nm over the whole measurement and treated with the different buffer solutions. The emission was obtained at 655 nm.

## 3.5 Sensor Film Measurement

### 3.5.1 Buffer Preparation

The pH value was adjusted with a digital pH meter (Seven Easy, Mettler Toledo) calibrated at 25 °C with standard buffers of pH 10.0, 7.0 and 4.0. The pH adjustments were done by using HCl (conc. or 1 M), NaOH (1 M) or diverse buffer substances.

### **3.5.2 Sensor Foils**

The sensor layer was knife-coated (12.5  $\mu\text{m}$  wet film thickness) onto a PET foil (Melinex 506/125  $\mu\text{m}$ ).

### **3.5.3 Optical Measurement**

Different methods were used for the optical measurement. The sensor membrane with the teflon filter was put in a homemade flow-through cell, which was flushed with different buffer solutions by a peristaltic pump. The buffer solutions and the measurement cell were held at a constant temperature of 23 °C. The spectra were recorded in front face mode with a FluoroLog®3 spectrofluorometer.

## **3.6 Chemical Treatment**

### **3.6.1 Hydrogenation**

For the hydrogenation a Parr Shaker Hydrogenation Apparatus was used as well as a Pyrex Reaction Bottle.

---

## 4 Experimental

### 4.1 Sensor Preparation - Hydrophobic System

#### 4.1.1 Buffer Solutions

##### TRIS Buffer

For a 20 mM TRIS buffer, 40 mL of a 1 M TRIS buffer solution were mixed with MilliQ and the pH value was adjusted to 7.4 with HCl (1 M). The buffer was then filled up with MilliQ to 2 L.

##### Ammonium chloride Buffers

For the ammonium chloride buffers a 3 M  $\text{NH}_4\text{Cl}$  solution was diluted. The exact amounts are listed in table 4.1. The amounts were taken and filled up to 50 mL with the TRIS buffer.

**Table 4.1:** Ammonium chloride amounts for 50 mL buffer solution

$\text{NH}_4\text{Cl}$ [mM]	[ $\mu\text{L}$ ] of 3 M $\text{NH}_4\text{Cl}$	[ $\mu\text{L}$ ] of 300 mM $\text{NH}_4\text{Cl}$
300	5000	
200	3333	
150	2500	
100	1667	
50		8333
25		4167
15		2500
10		1667
5		833
2		333

#### 4.1.2 Polymer/Plasticizer Cocktails

The used polymers in this section were polyvinyl chloride (PVC), ethyl cellulose (EC), cellulose acetate propionate (CAP), hydrothane 15 and hydrogel D4.

As plasticizer dioctyl sebacate (DOS), diethyl sebacate (DES), trioctyl phosphate (TOP), tributyl phosphate (TBP), triethyl phosphate (TEP) and trioctyl trimellitate (TOM) were used, as well as the ionic liquids 1-butyl-3-methylimidazolium hexafluorophosphate (BMIMPF<sub>6</sub>) and 1-butyl-3-methylimidazolium bis(trifluoromethylsulfonyl)imide (BMIIIm).

All cocktails were prepared with an amount of 10 wt.% of the polymer.

### Influence of Polymer Polarity - Cocktail Compositions

The composition of each tested cocktail is listed in table 4.2 for DOS as plasticizer and in table 4.3 for TBP as plasticizer. Additional to the listed additives, 60  $\mu\text{L}$  of a 2 mg/mL dye stock were added to each cocktail, which results in a concentration of 0.2 wt.% of the dye.

**Table 4.2:** Composition of polymer/DOS cocktails

Polymer	DOS [mg]	Polymer/ DOS ratio	Polymer [mg]	THF [ $\mu\text{L}$ ]
PVC	30	1/1	30	547
PVC	40	2/1	20	547
EC	0		60	547
EC	30	1/1	30	547
EC	40	2/1	20	547
CAP	30	1/1	30	547
CAP	40	2/1	20	547
Hydrothane 15	0		60	547
D4 (10 wt.%)	0		600	
D4 (10 wt.%)	30	1/1	300	300
EC (10 wt.%) in EtOH/Toluene 4/6	0		600	

**Table 4.3:** Composition of polymer/TBP cocktails

Polymer	TBP [mg]	Polymer/ TBP ratio	Polymer [mg]	THF [ $\mu\text{L}$ ]
PVC	30	1/1	30	547
PVC	40	2/1	20	547
EC	30	1/1	30	547
EC	40	2/1	20	547
CAP	30	1/1	30	547
CAP	40	2/1	20	547
D4 (10 wt.%)	30	1/1	300	300

#### 4.1.3 Lipophilic Ammonium Salts

For the preparation of the cocktails 4  $\mu\text{L}$  of a 2 mg/mL dye stock were mixed with 4 mL of the desired plasticizer. The resulting cocktail is divided in two halves. One half is mixed with 1 mL of ammonium octanoate or ammonium phenylacetate, respectively.

This results in two different cocktails:

- cocktail I: plasticizer + dye + salt
- cocktail II: plasticizer + dye

These cocktail were mixed together in different concentrations as follows:

- cocktail A: 400  $\mu$ L of cocktail II (0 % salt conc.)
- cocktail B: 80  $\mu$ L of cocktail I + 380  $\mu$ L of cocktail II (20 % salt conc.)
- cocktail C: 200  $\mu$ L of cocktail I + 200  $\mu$ L of cocktail II (50 % salt conc.)
- cocktail D: 400  $\mu$ L of cocktail I (100 % salt conc.)
- cocktail E: 400  $\mu$ L of cocktail II + 1 drop TFA

## 4.2 Sensor Preparation - Hydrophilic System

### 4.2.1 Polymer Studies - Composition of Cocktails

For the testing of hydrophilic polymers the ammonium chloride buffers from the hydrophobic part were used (0 mM, 100 mM and 300 mM) as well as 0.1 M HCl. Morpholinopolymer (MP) and different chain lengths of polyethylen glycol (PEG400, PEG100 and PEG3400) were used. The exact composition is shown in table 4.4.

**Table 4.4:** Composition of polymer cocktails used for polymer studies

polymer	polymer [mg]	buffer solvent [ $\mu$ L]
30 wt.% MP	150	350
10 wt.% MP	50	450
25 wt.% PEG	250	750
50 wt.% PEG	500	500
75 wt.% PEG	750	250

### 4.2.2 Buffer Solutions

#### BIS-TRIS Buffers - Internal Buffers

For a 1 M buffer, BIS-TRIS (2.09 g) was dissolved in MilliQ (5 mL), the solution was adjusted to the desired pH value (pH 6.0, 6.5 and 7.0) and then filled up to 10 mL. The buffer with pH 6.5 was then diluted to a buffercapacity of 100 and 10 mM BIS-TRIS.

#### Phosphate Buffer

For a 150 mM phosphate buffer,  $\text{NaH}_2\text{PO}_4$  (18 g) was dissolved in MilliQ (800 mL). The solution was adjusted to a pH value of 7.5 with 1 M NaOH and then filled up with MilliQ to 1 L.

## Amine Buffers

For the amine buffers appropriate amounts (see table 4.5) of different amines (ammonium chloride, trimethylammonium hydrochloride (TMA), dimethylamine hydrochloride (DMA) or methylamine hydrochloride (MA)) were dissolved in the phosphate buffer (150 mM, pH 7.5). The required amount of amine to get the appropriate free amine concentration was calculated using the Henderson-Hasselbalch equation with the respective  $pK_a$  value of the amine at a temperature of 23 °C.

**Table 4.5:** Amine amounts for 250 mL

free amine conc.		NH <sub>4</sub> Cl		TMA		DMA		MA	
[mg/L]	[mmol/L]	[mg]	[mmol]	[mg]	[mmol]	[mg]	[mmol]	[mg]	[mmol]
<b>0.3</b>	<b>0.018</b>	16	856	-	-	-	-	-	-
<b>0.5</b>	<b>0.03</b>	-	-	37	3536	-	-	-	-
<b>1</b>	<b>0.06</b>	52	2782	75	7168	398	32453	685	46251
<b>2.5</b>	<b>0.12</b>	143	7649	-	-	-	-	-	-
<b>5</b>	<b>0.3</b>	259	13854	370	35361	-	-	-	-
<b>10</b>	<b>0.6</b>	518	27708	740	70722	3975	324122	6850	462512
<b>20</b>	<b>1.2</b>	1036	55417	1479	141348	-	-	-	-

## pH Buffers

An universal buffer was used to perform pH cross sensitivity experiments.

Composition of the universal buffer for 20 mM and 100 mL:

- Citric acid monohydrate: 420 mg
- TRIS: 242 mg
- BIS-TRIS: 418 mg
- CAPS: 443 mg

The pH value was adjusted to pH 4.0 with HCl (1 M) and filled up with MilliQ to 100 mL. During the measurement the pH value was adjusted with NaOH (1 M) to pH 10.0.

For the determination of the  $pK_a$  value pH buffers without disturbing cations were required. Therefore appropriate amounts (see table 4.6) of different buffer substances were dissolved in MilliQ, brought to the desired pH value (with phosphoric acid, citric acid monohydrate or BIS-TRIS) and filled up with MilliQ to 100 mL resulting in a buffer capacity of 20 mM.

**Table 4.6:** pH Buffers

pH value	Buffer substance	mass [mg]
1.0	Hydrochloric acid	20
1.5	Phosphoric acid	20
2.5	Citric acid monohydrate	420
3.0	Citric acid monohydrate	420
3.5	Citric acid monohydrate	420
4.0	Citric acid monohydrate	420
4.5	Acetic acid	120
5.0	Acetic acid	120
5.5	Acetic acid	120
6.0	BIS-TRIS	418
7.0	BIS-TRIS	418

### 4.2.3 Cocktail Preparation

#### Polymer Cocktail

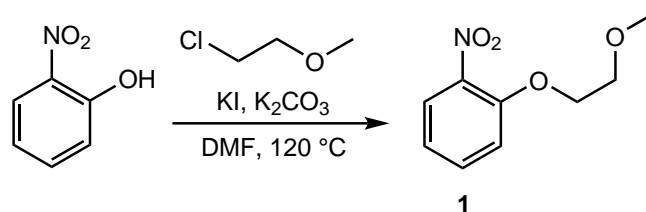
All polymer cocktails were prepared with an amount of 10 wt.% of the polymer. As polymer Hydrogel (Hydromed D1 and D4), polyhydroxypropyl methacrylate (PHPMA), polyhydroxyethyl methacrylate (PHEMA), polyethylene glycol (PEG), polyvinyl chloride (PVC), ethyl cellulose (EC) and celluloseacetate propionate (CAP) were used and as solvent either THF or a mixture of EtOH/BIS-TRIS buffer (9/1) was used.

#### Dye Cocktail

The dye cocktail consisted of the desired polymer cocktail and an indicator dye. The dye concentration of the cocktail was either 0.2 wt.% or 0.5 wt.% in respect to the polymer after drying. This dye cocktail was then knife-coated onto a PET foil.

### 4.3 Synthesis

#### 4.3.1 1-(2-Methoxyethoxy)-2-nitrobenzene (1)



**Figure 4.1:** Synthesis of compound **1**

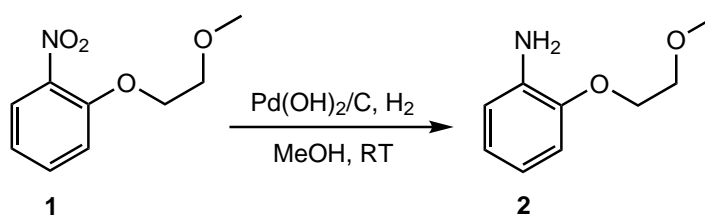
Nitrophenol (15.0 g, 107.8 mmol, 1.0 eq.) was dissolved in DMF (150 mL). 2-Chloroethylmethylether (16.7 mL, 183.3 mmol, 1.7 eq.),  $K_2CO_3$  (16.4 g, 118.6 mmol, 1.1 eq.) and KI (17.9 g, 107.8 mmol, 1.0 eq.) were added and the reaction mixture was stirred at 120 °C. After 6 hours TLC (C/EA 2/1) indicated complete consumption of the educt. The reaction mixture was allowed to cool to room temperature and filtered. DMF was evaporated, the residue was extracted with DCM and water, the organic layer was dried over  $Na_2SO_4$ , filtered and evaporated under high vacuum.

Yield: 21.17 g (99 %)

$^1H$ -NMR (300 MHz, Chloroform-d):  $\delta$  = 7.82 (d,  $J$  = 8.0 Hz, 1H), 7.51 (t,  $J$  = 7.8 Hz, 2H), 7.10 (d,  $J$  = 8.4 Hz, 1H), 7.03 (t,  $J$  = 7.7 Hz, 1H), 4.24 (t, 2H), 3.79 (t, 2H), 3.44 (s, 3H) ppm.

$^1H$ -NMR spectrum: figure 10.1 on page 67.

#### 4.3.2 2-(2-Methoxyethoxy)-aniline (2)



**Figure 4.2:** Synthesis of compound **2**

1-(2-Methoxyethoxy)-2-nitrobenzene (**1**) (10.0 g, 50.7 mmol, 1.0 eq.) was dissolved in MeOH (100 mL) in a Pyrex Reaction Bottle. A catalytic amount of  $Pd(OH)_2/C$  was added and the hydrogenation was done with a Parr Hydrogenation Apparatus. The reaction was finished, when no more hydrogen consumption was observed. (Reactiontime: 2 hours, TLC: C/EA 1/2,  $KMnO_4/H_2SO_4$ )



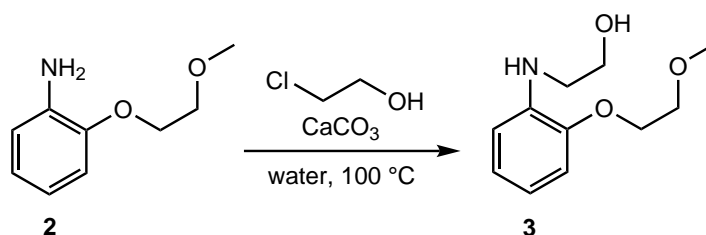
The reaction mixture was filtered and the solvent was removed under high vacuum.

Yield: 8.41 g (99 %)

$^1\text{H-NMR}$  (300 MHz, Chloroform-d):  $\delta = 6.90 - 6.77$  (m, 2H),  $6.77 - 6.64$  (m, 2H), 4.15 (t, 2H), 3.76 (t, 2H), 3.45 (s, 3H) ppm.

$^1\text{H-NMR}$  spectrum: figure 10.2 on page 68.

### 4.3.3 (((2-Methoxyethoxy)phenyl)amino)-ethanol (**3**)



**Figure 4.3:** Synthesis of compound **3**

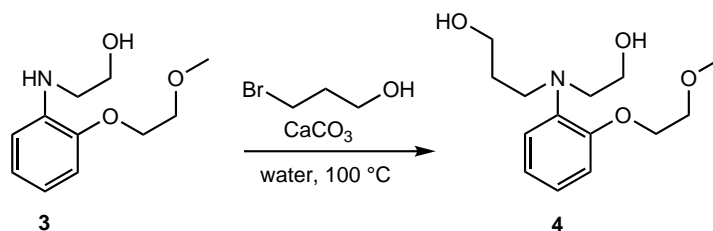
2-(2-Methoxyethoxy)-aniline (**2**) (8.3 g, 49.6 mmol, 1.0 eq.) was dissolved in  $\text{H}_2\text{O}$  dest. (80 mL). Chloroethanol (4.16 mL, 62.1 mmol, 1.25 eq.) and  $\text{CaCO}_3$  (7.45 g, 74.5 mmol, 1.5 eq.) were added and the reaction mixture was stirred at  $100\text{ }^\circ\text{C}$ . After one week GC-MS showed a 72 % conversion. The reaction mixture was allowed to cool to room temperature, filtered and washed with DCM. It was then extracted with DCM, water and brine and the organic layer was dried over  $\text{Na}_2\text{SO}_4$ , filtered and evaporated under high vacuum. The residue was purified via column chromatography on silica gel (C/EA 2/1 with a gradient to 1/5).

Yield: 5.3 g (51 %)

$^1\text{H-NMR}$  (300 MHz, Chloroform-d):  $\delta = 6.89$  (t,  $J = 7.4$  Hz, 1H), 6.81 (d,  $J = 7.7$  Hz, 1H), 6.67 (dd,  $J = 6.8, 3.8$  Hz, 2H), 4.13 (t, 2H), 3.76 (dt,  $J = 13.6, 4.7$  Hz, 4H), 3.43 (s, 3H), 3.31 (t, 2H) ppm.

$^1\text{H-NMR}$  spectrum: figure 10.3 on page 69.

#### 4.3.4 3-((2-Hydroxyethyl)(2-(2-methoxyethoxy)phenyl)amino)propan-1-ol (4)



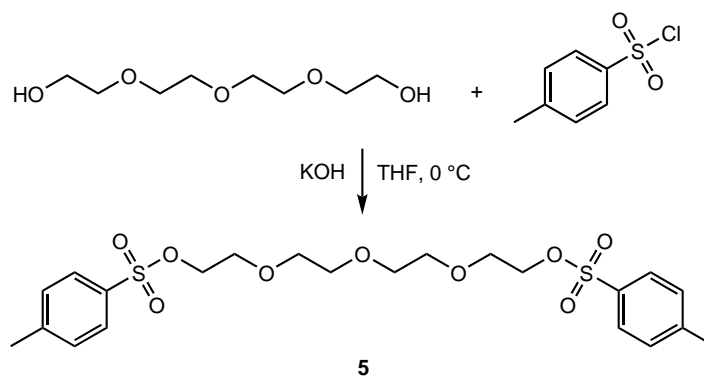
**Figure 4.4:** Synthesis of compound **4**

Compound **3** (5.3 g, 25.1 mmol, 1.0 eq.) was dissolved in  $\text{H}_2\text{O}$  dest. (20 mL). Bromopropanol (2.84 mL, 31.4 mmol, 1.25 eq.) and  $\text{CaCO}_3$  (3.77 g, 37.6 mmol, 1.5 eq.) were added and the reaction mixture was stirred at  $100\text{ }^\circ\text{C}$ . After 12 hours GC-MS showed a 83% conversion. The reaction mixture was allowed to cool to room temperature, filtered and washed with DCM. It was then extracted with DCM, water and brine and the organic layer was dried over  $\text{Na}_2\text{SO}_4$ , filtered and evaporated under high vacuum. (TLC: EA)

Yield: 4.24 g (58%)

$^1\text{H-NMR}$  (300 MHz, Chloroform- $d$ ):  $\delta = 9.17 - 9.08$  (m, 1H),  $9.06 - 8.98$  (m, 1H),  $8.96 - 8.81$  (m, 2H),  $6.09$  (t,  $J = 6.9, 5.7$  Hz, 2H),  $5.75$  (t, 2H),  $5.70$  (t,  $J = 5.5$  Hz, 2H),  $5.59 - 5.51$  (m, 2H),  $5.40$  (s, 3H),  $5.21$  (t,  $J = 6.1$  Hz, 2H),  $5.10 - 5.02$  (m, 2H),  $3.70 - 3.57$  (m, 2H) ppm.  
 $^1\text{H-NMR}$  spectrum: figure 10.4 on page 70.

#### 4.3.5 Tetraethylene glycol ditosylate (5)



**Figure 4.5:** Synthesis of compound **5**

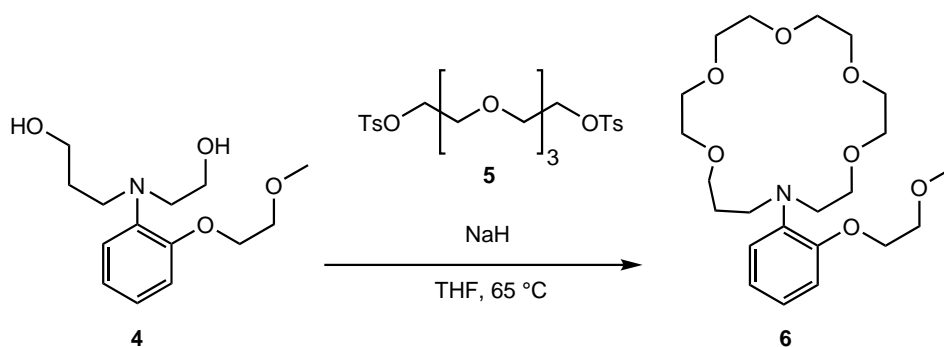
Tetraethylene glycol (8.8 mL, 56.6 mmol, 1.0 eq.) was dissolved in THF (50 mL). The reaction mixture was cooled to 0 °C and then KOH (12.0 g, 213.9 mmol, 3.8 eq.) was added. Afterwards a solution of p-toluenesulfonyl chloride (23.8 g, 124.6 mmol, 2.2 eq) in THF (50 mL) was added dropwise over a period of 90 minutes. The reaction mixture was stirred at 0 °C for 4 hours and then at room temperature overnight. The resulting suspension was filtered and the solvent was removed under high vacuum. The residue was purified via column chromatography on silica gel (C/EA 4/1 with a gradient to 1/2).

Yield: 15.03 g (53 %)

<sup>1</sup>H-NMR (300 MHz, Chloroform-d):  $\delta$  = 7.77 (d, J = 8.1 Hz, 4H), 7.32 (d, J = 8.0 Hz, 4H), 4.15 (t, 4H), 3.67 (t, 4H), 3.54 (s, 8H), 2.42 (s, 6H) ppm.

<sup>1</sup>H-NMR spectrum: figure 10.5 on page 71.

#### 4.3.6 NH<sub>4</sub><sup>+</sup> Crown (6)



**Figure 4.6:** Synthesis of compound 6

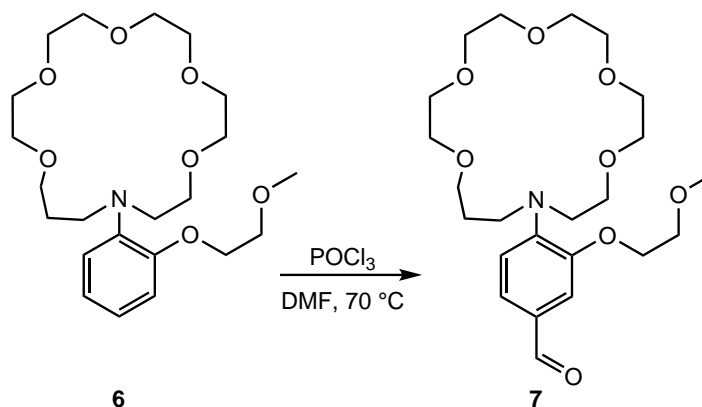
In a flame dried and argon flushed Schlenk flask compound 4 (3.5 g, 13 mmol, 1.0 eq.) was dissolved in dry THF (15 mL) and then NaH (1.14 g, 28.6 mmol, 2.2 eq.) was added. The reaction mixture was heated to 65 °C. Tetraethylene glycol ditosylate (5) (6.53 g, 13 mmol, 1.0 eq.) in dry THF (20 mL) was added dropwise over a period of 90 minutes. The reaction mixture was stirred overnight. After 12 hours TLC (DCM/MeOH 15/1, CAM) indicated full conversion. The solution was allowed to cool to room temperature and filtered. The solvent was removed and the residue was extracted with DCM, water and brine. The organic layer was dried over Na<sub>2</sub>SO<sub>4</sub>, filtered and the solvent was removed under high vacuum. Purification was done via column chromatography on silica gel (DCM/MeOH with a gradient from 0.5 % MeOH to 5 % MeOH).

Yield: 3.49 g (63 %)

$^1\text{H-NMR}$  (300 MHz, Chloroform-d):  $\delta = 6.97$  (d,  $J = 7.2$  Hz, 1H), 6.91 – 6.80 (m, 3H), 4.08 (t, 2H), 3.72 (t, 2H), 3.53 (d,  $J = 13.0$  Hz, 18H), 3.45 – 3.41 (m, 2H), 3.39 (s, 3H), 3.30 (t, 2H), 3.23 (t, 2H), 1.76 – 1.62 (m, 2H) ppm.

$^1\text{H-NMR}$  spectrum: figure 10.6 on page 72.

#### 4.3.7 $\text{NH}_4^+$ Crown Aldehyde (7)



**Figure 4.7:** Synthesis of compound 7

In a flame dried and argon flushed Schlenk flask compound **6** (750 mg, 1.75 mmol, 1.0 eq.) was dissolved in dry DMF (4 mL). POCl<sub>3</sub> (1.6 mL, 17.5 mmol, 10 eq.) was added at a temperature of -10 °C. After 12 hours of stirring the reaction mixture was heated to 70 °C for one hour and after TLC control (DCM/MeOH 10/1, Dinitrophenylhydrazine) the reaction mixture was slowly poured over ice and stirred for another 10 minutes. It was neutralized with Na<sub>2</sub>CO<sub>3</sub> and then extracted with DCM and water. The organic layer was dried over Na<sub>2</sub>SO<sub>4</sub>, filtered and the solvent was removed under high vacuum. The purification was done via column chromatography on silica gel (DCM/MeOH with a gradient from 0.5 % MeOH to 10 % MeOH).

Yield: 100 mg (13 %)

$^1\text{H-NMR}$  (300 MHz, Chloroform-d):  $\delta = 9.83 - 9.65$  (m, 1H), 7.41 – 7.23 (m, 1H), 7.03 – 6.81 (m, 2H), 4.22 – 4.03 (m, 2H), 3.79 – 3.70 (m, 2H), 3.65 – 3.41 (m, 22H), 3.39 (s, 3H), 3.37 – 3.18 (m, 2H), 1.92 – 1.60 (m, 2H) ppm.

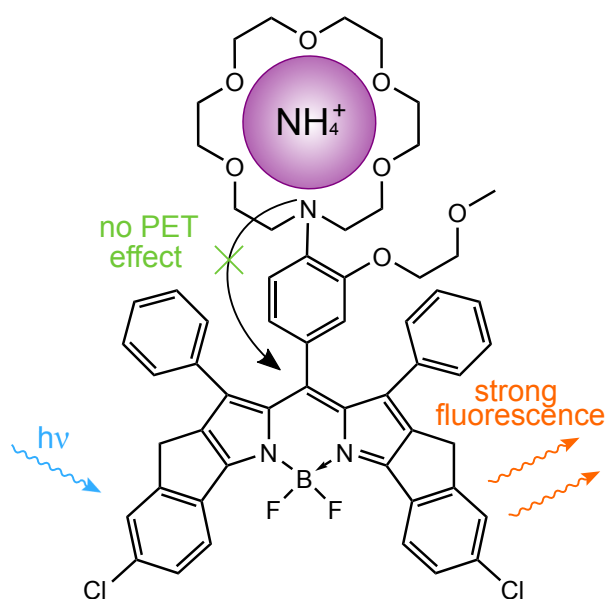
$^1\text{H-NMR}$  spectrum: figure 10.7 on page 73.

---

## 5 Results and Discussion

### 5.1 Scope of this Thesis

The aim of this thesis was the development of a novel method for the optical detection of ammonia. The concept is based on fluoroionophores which are capable of detecting ammonium ions. The fluoroionophore which was chosen, and the working principle, is shown in figure 5.1.



**Figure 5.1:**

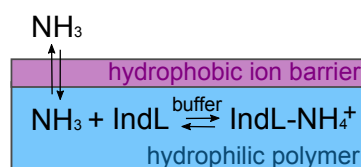
Fluoroionophore - FI3

If an ammonium ion occupies the cavity of the crown ether no PET effect occurs, therefore, a strong fluorescence is observed.

The decision to use this compound is based on the work of Bernhard Müller. [2] In the mentioned paper a potassium selective fluoroionophore is presented, which shows a cross sensitivity to ammonium ions. This is due to the fact that the  $\text{K}^+$ - and the  $\text{NH}_4^+$ -ion have a similar diameter (potassium: 2.66 Å, ammonium: 2.68 Å) and both ions fit perfectly into the crown ether (cavity diameter: 2.6-3.2 Å).

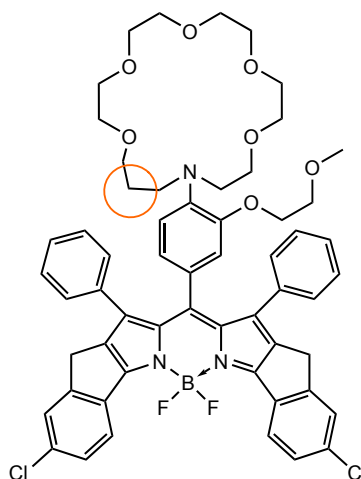
This thesis consists of three parts. The first part will discuss **hydrophobic matrices**, with the idea to immobilize the fluoroionophore in it. First of all, solvent and polymer studies have been performed. Afterwards, it was tried to prepare a solid state sensor for ammonia. For this setup the sensor can be covered with an ion impermeable layer to prevent a response to ionic species ( $K^+$ ), but ammonia can still diffuse through this protection layer. As the indicator dye is not sensitive to ammonia, an acid is required in the sensor system to generate the corresponding ammonium ion. Therefore, an acid concentration screening in combination with a plasticizer screening was done. The detailed studies are discussed in section 5.2.

The second part of this thesis is based on the same concept, but instead of hydrophobic matrices **hydrophilic** ones were used. Again, the ammonium ion has to be generated in the sensor system and in this case an internal buffer solution was used. The setup of the sensor system is shown in figure 5.2. The detailed studies are discussed in section 5.3.



**Figure 5.2:**  
Sensor setup for hydrophilic matrices

The third part of the thesis was the synthesis of an optimized crown ether and further the fluoroionophore with this new receptor. The idea was to increase the diameter of the cavity of the crown ether and subsequently the fluoroionophore with this receptor via adding an additional  $CH_2$ -group to the crown. Thus, the crown should be too big for the  $K^+$ -ion and in consequence maybe more sensitive to ammonium. The optimized FI is shown in figure 5.3.

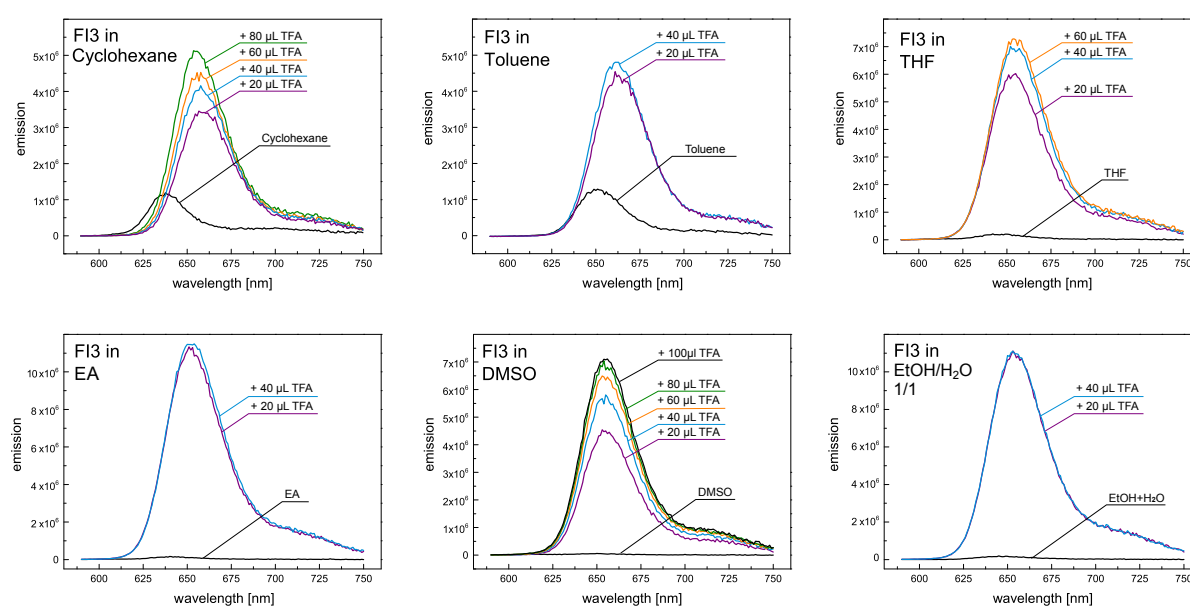


**Figure 5.3:**  
Structure of an optimized fluoroionophore for the detection of ammonium.

## 5.2 Part 1: Hydrophobic Matrices

### 5.2.1 Influence of Solvent Polarity to the PET Efficiency

Fluoroionophore based optical sensing relies on the principle of the PET effect, which is a redox reaction in the excited state of a fluoroionophore, as described in section 2.3.3. This reaction is highly influenced by its environment. For this reason, the influence of the polarity of different solvents on the PET efficiency of the fluoroionophore was investigated. Therefore, 30  $\mu\text{L}$  of a 50  $\mu\text{L}/\text{mL}$  FI3 stock solution together with the respective solvent are mixed in a cuvette and measured with a spectrofluorometer to obtain a baseline. After measuring the baseline, trifluoroacetic acid (TFA) was added to the solution and it was measured again. In figure 5.4 the obtained data are illustrated.



**Figure 5.4:**

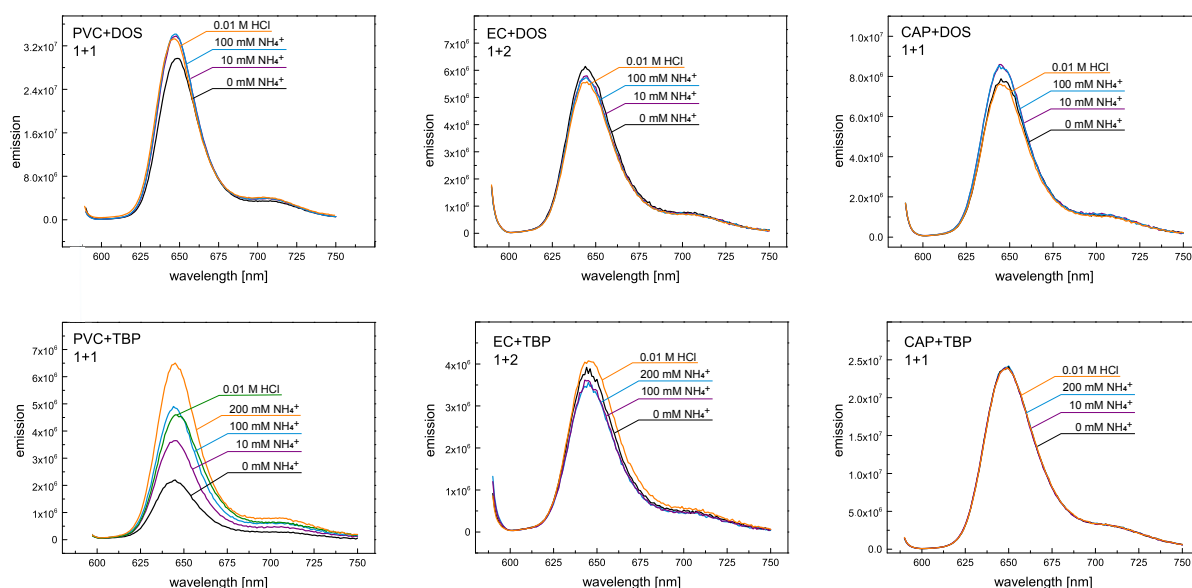
Solvent testing:

Increasing polarities of the solvents from the left top to the right bottom picture.

The PET effect is typically stronger in more polar solvents and is weakened in an apolar environment. In this study, the same trend of PET efficiencies in different polarities could be obtained. The conclusion is, that a fluoroionophore in a hydrophobic (non-polar) medium is already fluorescent. That means that a complexation with ions does not lead to a significant increase in emission in contrast to a polar medium, where a sufficient PET quenching takes place.

### 5.2.2 Influence of Polymer Polarity on the PET Efficiency

As the indicator dye needs to be immobilized in a polymer matrix, the influence of various polymers (both hydrophobic and hydrophilic) was investigated. In addition to the polymer, the plasticizers dioctyl sebacate (DOS) and tributyl phosphate (TBP) were immobilized in the matrix to gain a better mobility for the ions within the hydrophobic system. As polymer polyvinyl chloride (PVC), ethyl cellulose (EC) and celluloseacetate propionate (CAP) were used. Sensor foils were prepared and measured with a spectrofluorometer at a right angle mode. The foils were first conditioned with phosphate buffer to obtain a baseline. Afterwards they were measured with different concentrations of ammonium buffer. The exact composition of the measured sensor foils can be found in section 4.1.2 at page 28. The most significant spectra are shown in figure 5.5 and 5.6.



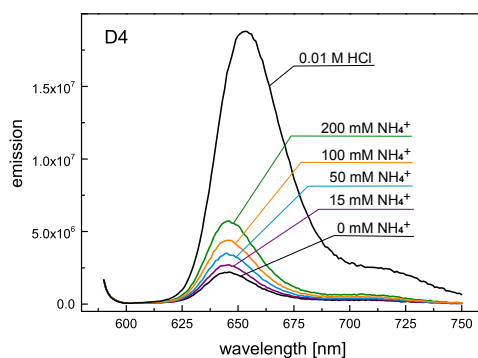
**Figure 5.5:**

Polymer testing:

The three pictures in the first row show the different polymers with DOS as plasticizer, in the second row the same polymers were used but with TBP instead of DOS as plasticizer.

In general, hydrophobic matrices did not show any response to ammonium ions. This means that either the fluoroionophore is already in the "on"-state without ions or that the ion mobility is too low within the matrices used in figure 5.5. Additionally, HCl was not able to protonate the sensor membrane. This could be explained by the high dilution of the used acid. However, if a hydrophilic matrix (e.g. Hydrogel D4) is used it is possible to obtain a fluorescence increase with aqueous ammonia solutions and also protonation can be achieved as shown in figure 5.6.





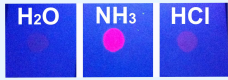

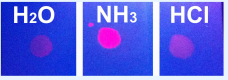
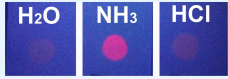
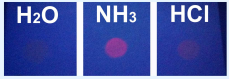
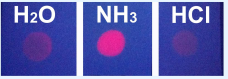
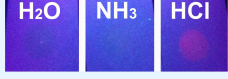


**Figure 5.6:**  
Polymer testing:  
Hydrogel D4 was used as polymer without a plasticizer.

### 5.2.3 Plasticizer and Acid Concentration Screening

If there is a protective layer used for the sensor, an acid is required inside the membrane in order to generate the corresponding ammonium ion. This acid must fulfill several requirements. The  $pK_a$  value should be between 5 and 6 and it should not protonate the crown, which has a  $pK_a$  between 3 and 4. Additionally, the acid must be lipophilic so it is not prone to leaching out of the hydrophobic matrix into hydrophilic samples. Concerning these parameters, octanoic acid was chosen, which has a  $pK_a$  of 4.89. Due to the results of the polymer testing, it was decided to just use plasticizers without hydrophobic matrices as it was not possible to obtain any measurable signal increase with these matrices when treated with ammonia or acid.

The acid concentration screening was performed with different plasticizers, such as TBP, DOS and trioctyl phosphate (TOP) and further on with ionic liquids (IL). [30]

The plasticizer was mixed with 100 to 200  $\mu\text{L}$  of a 2 mg/mL dye stock and different equivalents of octanoic acid. From each solution three drops were taken and each of them was dropped on a separate filter paper. One of the filter papers was then exposed to  $\text{H}_2\text{O}$  vapor, one to  $\text{NH}_3$  vapor and the last one to  $\text{HCl}$  vapor. Afterwards they were exposed to UV light and have been photographed. The results are shown in figure 5.7 and 5.8.

Acid	180 eq.	360 eq.	900 eq.
DOS			
TOP			
Acid	270 eq.	550 eq.	2730 eq.
TBP			

**Figure 5.7:**


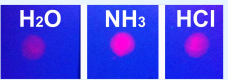
Plasticizer testing:

DOS, TOP and TBP were used as plasticizers. The equivalents of octanoic acid are shown in the figure. The filter paper was exposed to the vapor phase of H<sub>2</sub>O, NH<sub>3</sub> or HCl.

It was expected that the fluorescence is in the "off"-state if the sensor is in presence of water vapor. However, when treated with NH<sub>3</sub> vapor an increase of the fluorescence is observed. If the sensor system is presented to HCl vapor it should be completely protonated and, therefore, a high intensity of fluorescence should be obtained.

With increasing acid concentration inside the sensor it gets more and more protonated and therefore even in the H<sub>2</sub>O vapor, fluorescence is expected. The experimental results were like the expected ones except when the sensor system was presented to HCl.

The presented data show, that NH<sub>3</sub> and HCl show a similar increase of fluorescence which is surprising. However, as real intensity measurements were not performed it is difficult to distinguish between the real intensities. This results are promising as NH<sub>3</sub> vapor showed a turn "on"-effect of the sensor.

Acid	90 eq.	Acid	190 eq.
BMIIm		BMIMPF6	

**Figure 5.8:**

Ionic liquid testing:

1-butyl-3-methylimidazolium bis(trifluoromethylsulfonyl)imide (BMIIm) and 1-butyl-3-methylimidazolium hexafluorophosphate (BMIMPF6) were used.

As can be seen in figure 5.8, the sensor system was already in the "on"-state without treating it with the analyte. This could be due to a very polar environment, which inhibits the PET effect.

### 5.2.4 Using Lipophilic Ammonium Salts

In general, to gain a suitable signal ammonia first has to diffuse within the sensor system to the acid to form the ammonium ion. After this step, the ammonium has to diffuse to the crown. As there are many unknown processes, the idea behind this section was to implement ammonium salts in the sensor system to overcome the first diffusion step.

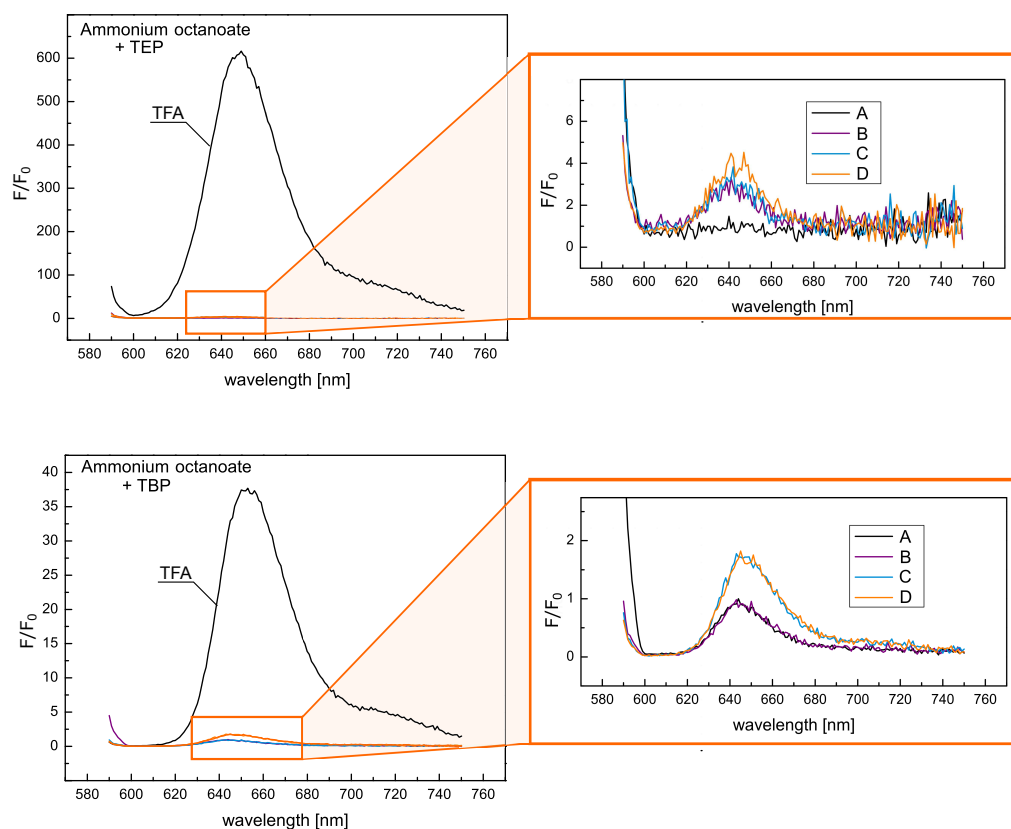
Two salts were first produced and then tested (ammonium octanoate and ammonium phenylacetate). For the testing, different concentrations of salts were dissolved in different plasticizers such as DOS, TBP, TOP, trioctyl trimellitate (TOM), diethyl sebacate (DES) and triethyl phosphate (TEP). One test was also made with the ionic liquid BMIMPF<sub>6</sub> as shown in table 5.1.

**Table 5.1:** Solubility of salts in plasticizers and obtained spectra

Plasticizer	Ammonium octanoate		Ammonium phenylacetate	
	Solubility	Spectra	Solubility	Spectra
DOS	x	x	x	x
BMIMPF <sub>6</sub>	x	x	x	x
TOM	x	x	x	x
DES	✓ at 80 °C	x	✓ at 60 °C	x
TOP	✓ at 80 °C	x	x	x
TBP	✓ at 60 °C	✓	✓ at 40 °C	✓
TEP	✓	✓	✓	✓

The solubility of the salts was limited, therefore it was not possible to measure spectra of each one, but as shown in table 5.1 spectra for TBP and TEP could be obtained.

The spectra were measured in solution with a 1 mm cuvette on the Fluorolog in front face mode. The composition of the salt-dye cocktails, which were used to measure the spectra in figure 5.9, is written in section 4.1.3 on page 28 of the experimental chapter.



**Figure 5.9:**

Ammonium octanoate with TEP (upper spectra) and TBP (lower spectra) with the corresponding closeup views.

A = 0 % of salt-dye cocktail, B = 20 % of salt-dye cocktail  
 C = 50 % of salt-dye cocktail, D = 100 % of salt-dye cocktail

The spectra for ammonium phenyl acetate looked similar to the spectra which are shown in figure 5.9. As can be seen, there is no high influence on the fluorescence with increasing ammonium salt concentration. However, it could also be that the ammonium ion is already very stabilized by its lipophilic counter ion. As no satisfying sensor was obtained using the highly complex hydrophobic matrix systems, it was decided to also investigate hydrophilic matrices. The disadvantage of hydrophilic polymers is that the ammonium ion does not need to be stabilized in a crown ether as the polar environment of the matrix already stabilizes the ion. Due to that, it is expected that in hydrophilic matrices a lower sensitivity is obtained.

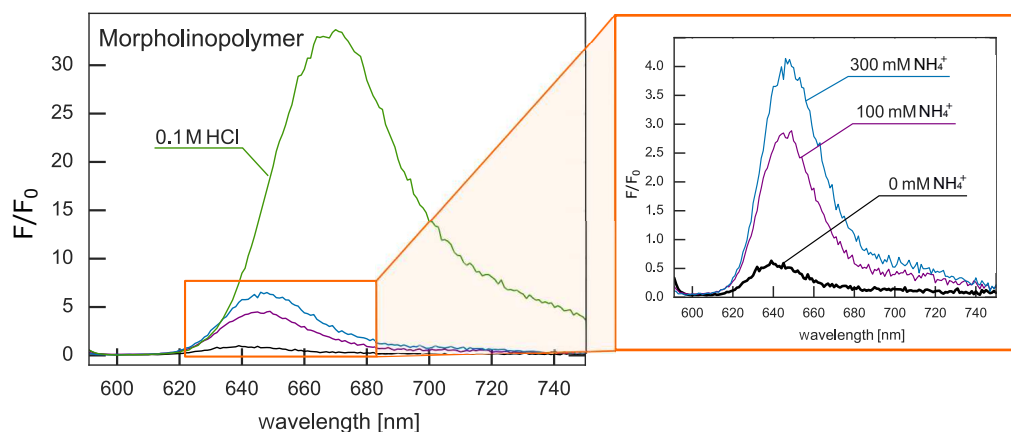
## 5.3 Part 2: Hydrophilic Matrices

### 5.3.1 Polymer Studies

Due to the fact that the initial studies to immobilize the fluoroionophore in a hydrophobic matrix did not lead to a functional sensor, hydrophilic matrices were tested.

First of all, a hydrophilic polymer testing was done. Therefore the required concentration of the polymer was added to buffer solutions with different concentrations of  $\text{NH}_4^+$  (100 mM and 300 mM) and to a solution of 0.1 M HCl. The exact composition of the cocktails is listed in section 4.2.1 on page 29 in the experimental chapter.

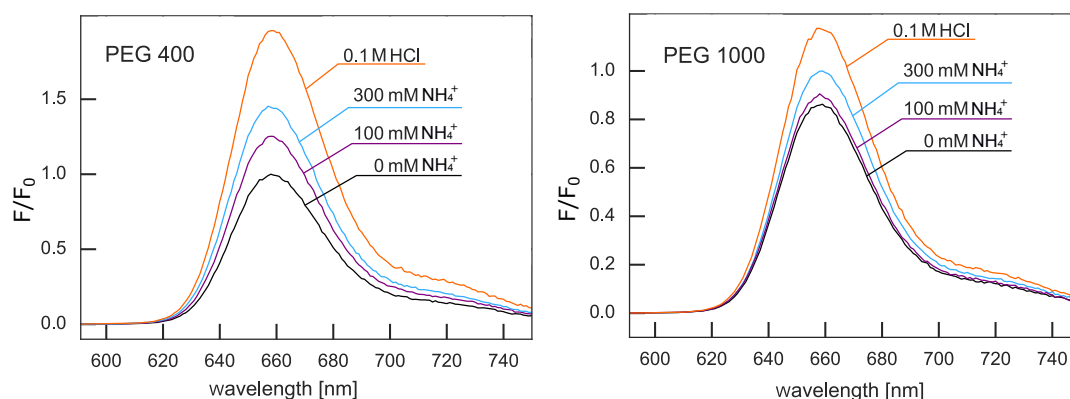
The spectra of the cocktails were measured on the Fluorolog in front face mode. Some of the obtained spectra are shown in the figures 5.10, 5.11 and 5.12.



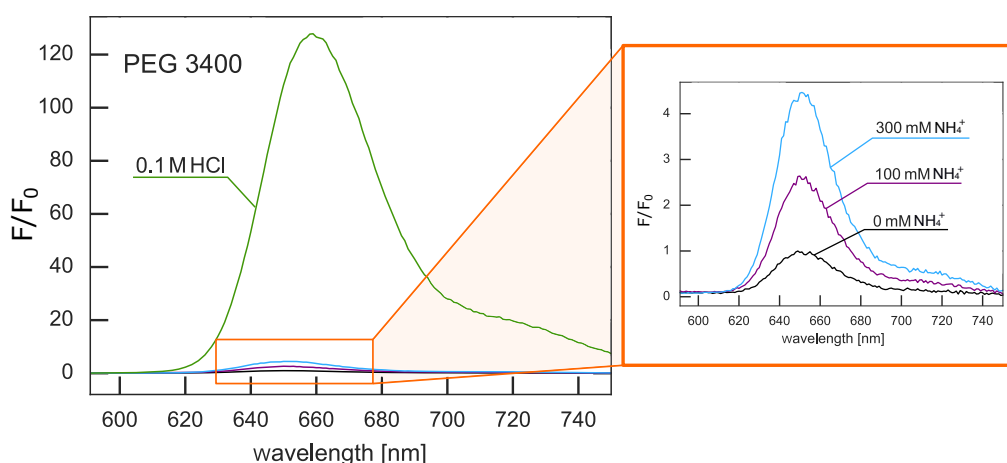
**Figure 5.10:**

10 wt.% Morpholinopolymer knife-coated on PET foil.

This polymer showed a good response to the analyte. The signal, which was obtained was four times higher at a concentration of 300 mM  $\text{NH}_4^+$ .



**Figure 5.11:**  
75 wt.% PEG knivecoated on PET foil  
left: PEG 400, right: PEG 1000  
The response to lower PEG chains was not sufficient.



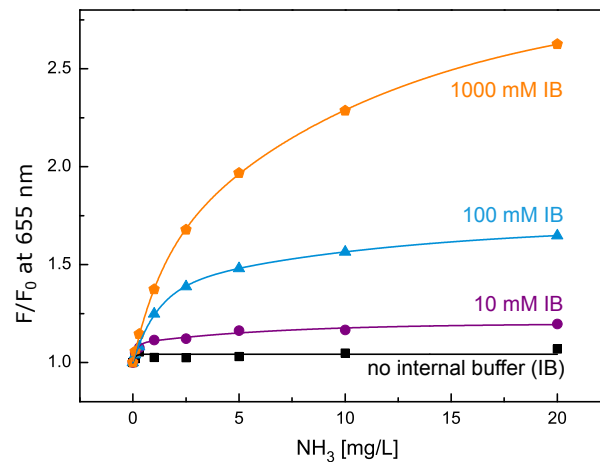
**Figure 5.12:**  
50 wt.% PEG 3400 knivecoated on PET foil  
A longer PEG chain obtained a good fluorescence increase.

As discussed, hydrophilic polymers show a response to the ammonium ion. However, PEG or morpholino-based materials did not show a major improvement of the response compared to the well-known polyurethane hydrogels. This hydrogels (for example D1 or D4) are commonly used for pH or ion sensing and show a good response to ammonia (figure 5.6). For this reasons, it was attempted to develop an ammonia sensor based on hydrogel D1.

### 5.3.2 Influence of Internal Buffer

As hydrophilic matrices can uptake water, it is necessary to adjust the pH within the sensor membrane in order to facilitate the generation of ammonium. For this reason, the decision was made to use BIS-TRIS ( $pK_a=6.5$ ) as internal buffer, because it has a high solubility in hydrogel. Additionally, it is necessary to cover the sensor layer with a hydrophobic protective layer to prevent penetration of charged species such as protons or ions. Therefore, a teflon membrane which is highly permeable for ammonia was used. The influence of each parameter will be discussed in more detail in the following sections.

The calibration of the sensor foil was done in a home-made flow-through cell on the Fluorolog in the front face mode.



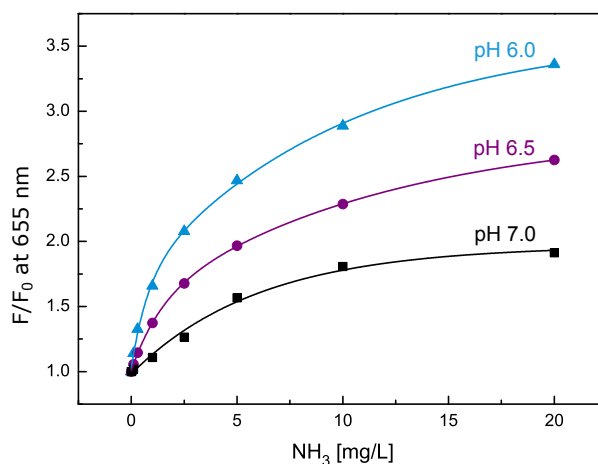
**Figure 5.13:**

Influence of the internal buffer capacity with an pH value of 6.5.

The calibration curves in figure 5.13 show the influence of different buffer capacities on the sensor. Ammonia has to diffuse through the ion protective layer and afterwards the ammonium ions have to be generated to gain a signal. For the generation of the ions an internal buffer is required. A non buffered system does not show any response, due to the fact that without an internal buffer no ammonium can be generated. If the buffer capacity is increased the response of the sensor is increased, because with more internal buffer, more ammonium ions can be generated. For further measurements the 1000 mM BIS-TRIS buffer system was chosen.

### 5.3.3 Influence of Internal pH Value

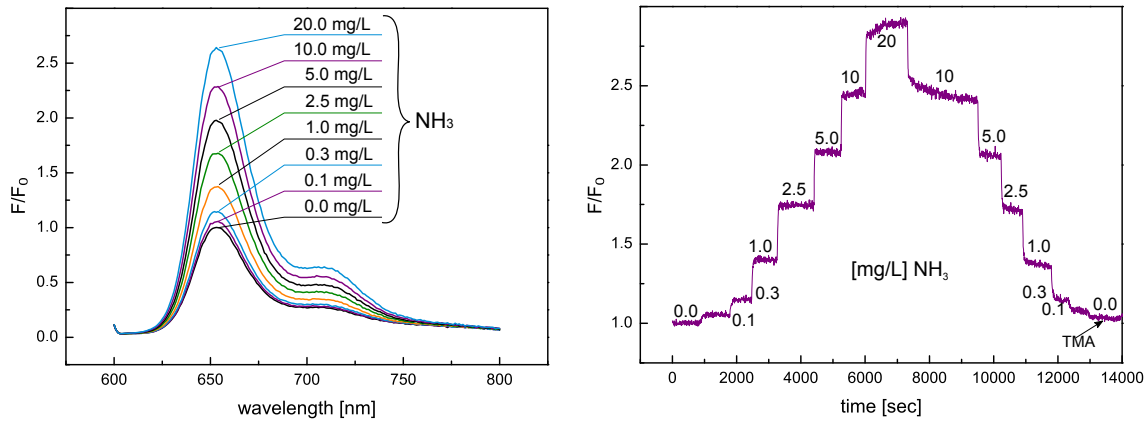
According to the Henderson-Hasselbalch equation the lowest possible pH value was intended to favor the protonation of  $\text{NH}_3$ . Generally the lower the pH value, the more  $\text{NH}_4^+$  is generated and according to that, the fluorescence is increased. A problem occurs if the pH value is too low. If this happens, the crown ether itself could be protonated. A protonation of the crown disturbs the PET effect and the fluorescence is increased. In figure 5.14 the obtained calibration curves for different pH values (pH 6.0, 6.5 and 7.0) are illustrated. The sensor setup and measuring mode was the same as for the buffer capacity measurements.



**Figure 5.14:**  
Calibration curve, which shows the influence of the internal pH value.

If the fluoroionophore (FI3) is immobilized in hydrogel D1 a  $\text{pK}_a$  value of 3.2 is obtained, which means that a minor amount of the receptor can already be protonated at a pH of 6.0. This results in a fluorescence emission even in the absence of ammonium. In concern of this aspects an internal pH value of 6.5 was used for the further investigations. Due to the increase of the pH value, no protonation of the receptor occurs by the buffer. In figure 5.15 the emission and kinetic spectra are shown for the sensor setup with an internal buffer of 1000 mM BIS-TRIS and pH 6.0.



**Figure 5.15:**

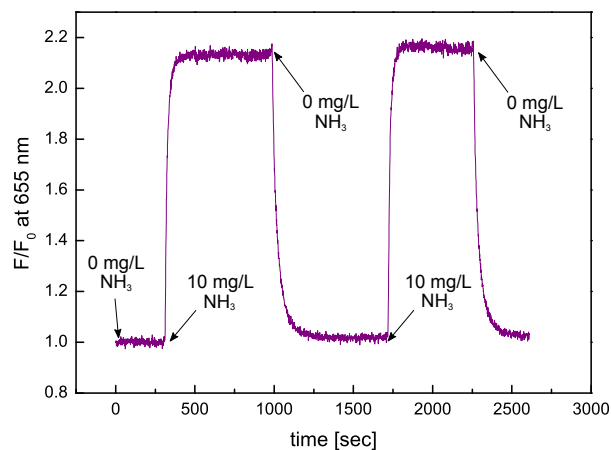
Emission spectra is shown on the left side and kinetic spectra on the right side. Measurements with an internal buffer 1000 mM and pH 6.0

### 5.3.4 Hysteresis and Response Times

In concern to the previous tests, the ideal sensor system for now is the following:

- 0.5 wt.% dye in
- 10 wt.% D1 polymer cocktail in EtOH/buffer 9/1 with
- buffer: BIS-TRIS, 1000 mM, pH 6.5
- and teflon filter as protection layer

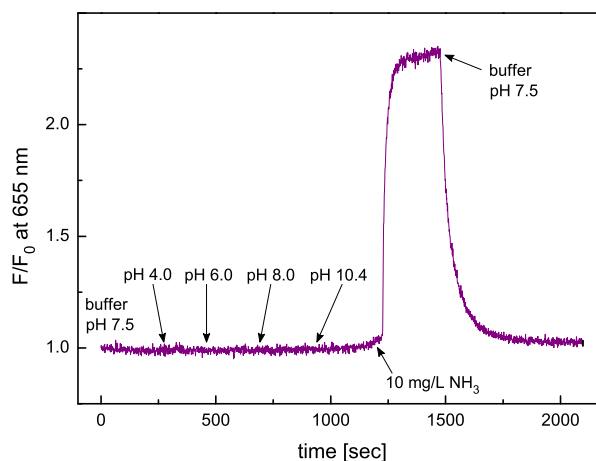
All of the following tests were made with this sensor system and measured on the Fluorolog with the home-made flow-through cell via front face mode. Figure 5.16 illustrates that the sensor response is between 1 and 3 minutes and is fully reversible. Additionally, no major hysteresis or drift is visible.

**Figure 5.16:**

Response and recovery times of sensor system to ammonia and buffer solution

### 5.3.5 Cross Sensitivity to different pH Values of the Sample

In this section, the cross sensitivity of the sensor system to different pH values in the sample is described. Concerning real-world applications, it is very important that the sensor is inert to changes of the pH of the sample. The obtained spectra is shown in figure 5.17. For the determination of this spectra an universal buffer was pumped through the measuring cell. It was adjusted with NaOH (1 M).

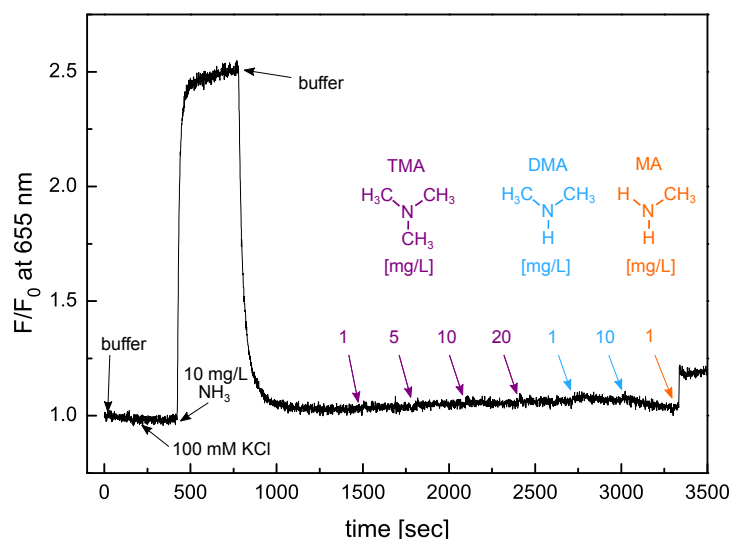


**Figure 5.17:**  
pH dependency of the sensor system

Due to the teflon filter which covers the sensor, there is no response of the sensor system to pH changes. However, 10 mg/L  $\text{NH}_3$  can diffuse through the teflon membrane and show the expected signal increase.

### 5.3.6 Cross Sensitivity to other Amines and Potassium

The main improvement of this sensor system was, that it should not be sensitive to other amines, contrary to state-of-the-art ammonia sensors. Therefore, a testing of the cross sensitivity to other amines was of high interest. Trimethylamine (TMA), dimethylamine (DMA) and methylamine (MA) were tested. A KCl solution was also tested to illustrate the effectivity of the hydrophobic teflon protective membrane.



**Figure 5.18:**

Cross sensitivity to other amines (TMA, DMA, MA) and potassium.

As expected, the sensor system did not show any response to potassium, because of the teflon filter, which prevents the diffusion of other ions into the membrane. Due to the working principle of the sensor, which is based on the complexation of ammonium, trimethylamine and dimethylamine did not show any response as well. This is because they are too bulky to fit in the cavity of the crown ether. However, the sensor responded to methylamine, which can be seen in figure 5.18. The reason of this response is, that the one methyl group on the ammonium ion can arrange itself to be outside of the crown ether, whilst the other two hydrogens are small enough to be complexed. This interference could be overcome by using a cryptand receptor to enhance the sterical hindrance.

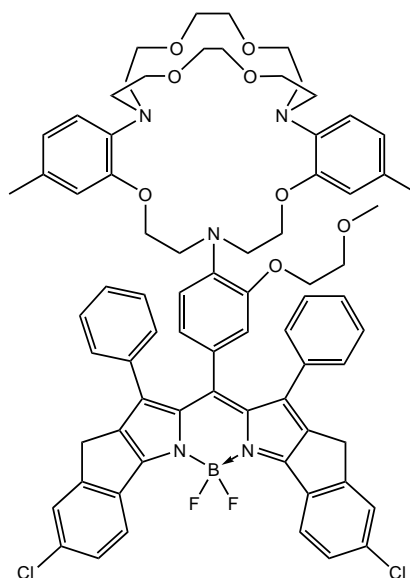
However, this results are very promising as, for example, in the fish farming industry, there is a high interest in measuring trimethylamine. It is a degradation product of fish and therefore, occurs in high concentrations. Currently available optical ammonia sensors can not distinguish between ammonia and trimethylamine.

### 5.3.7 Further Investigations

As a good sensor system and a general understanding of the working principle was obtained, further investigations were attempted.

#### Using a more Sensitive Fluoroionophore

The idea was to use a cryptant instead of a crown ether, because of the sterically more protected cavity. In this particular case a triazacryptand (TAC), which was developed by He et al. was chosen. [31] It is known, that the TAC-BODIPY fluoroionophore shows a good response to the ammonium ion in solution.



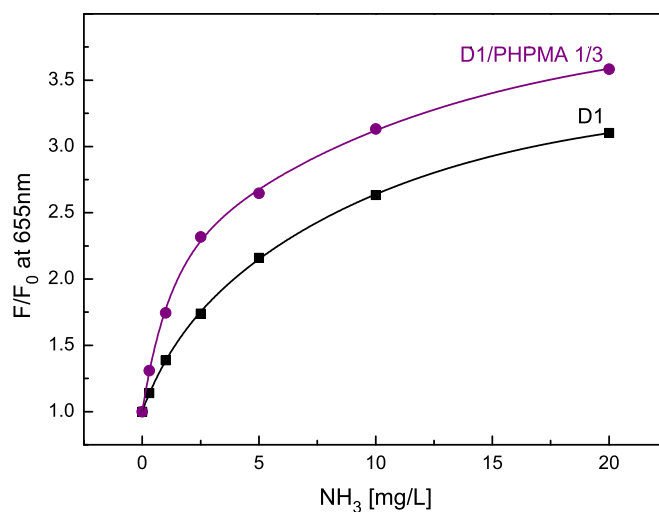
**Figure 5.19:**  
TAC-BODIPY fluoroionophore

After embedding the TAC-BODIPY fluoroionophore into the well working sensor system, measurements with the Fluorolog were done. Unfortunately no response was obtained. Briefly, it is expected that the TAC receptor is too hydrophobic and, therefore, accumulates in the hydrophobic domains of the hydrogel and, hence, is not available for complexation with the analyte. Detailed studies can be found in the master's thesis of Tanja Rappitsch. [32]

Another idea was to improve the crown ether via adding an additional  $\text{CH}_2$ -group to the crown. This procedure is described in section 5.4.

### Polymer Investigation

Due to the fact that the tests with the triaza-cryptand-ionophore did not show the desired effect, it was attempted to change the polarity within the polymer to enhance the stability of the binding. Therefore, polyhydroxy propyl methacrylate (PHPMA) as additional polymer compound was used.



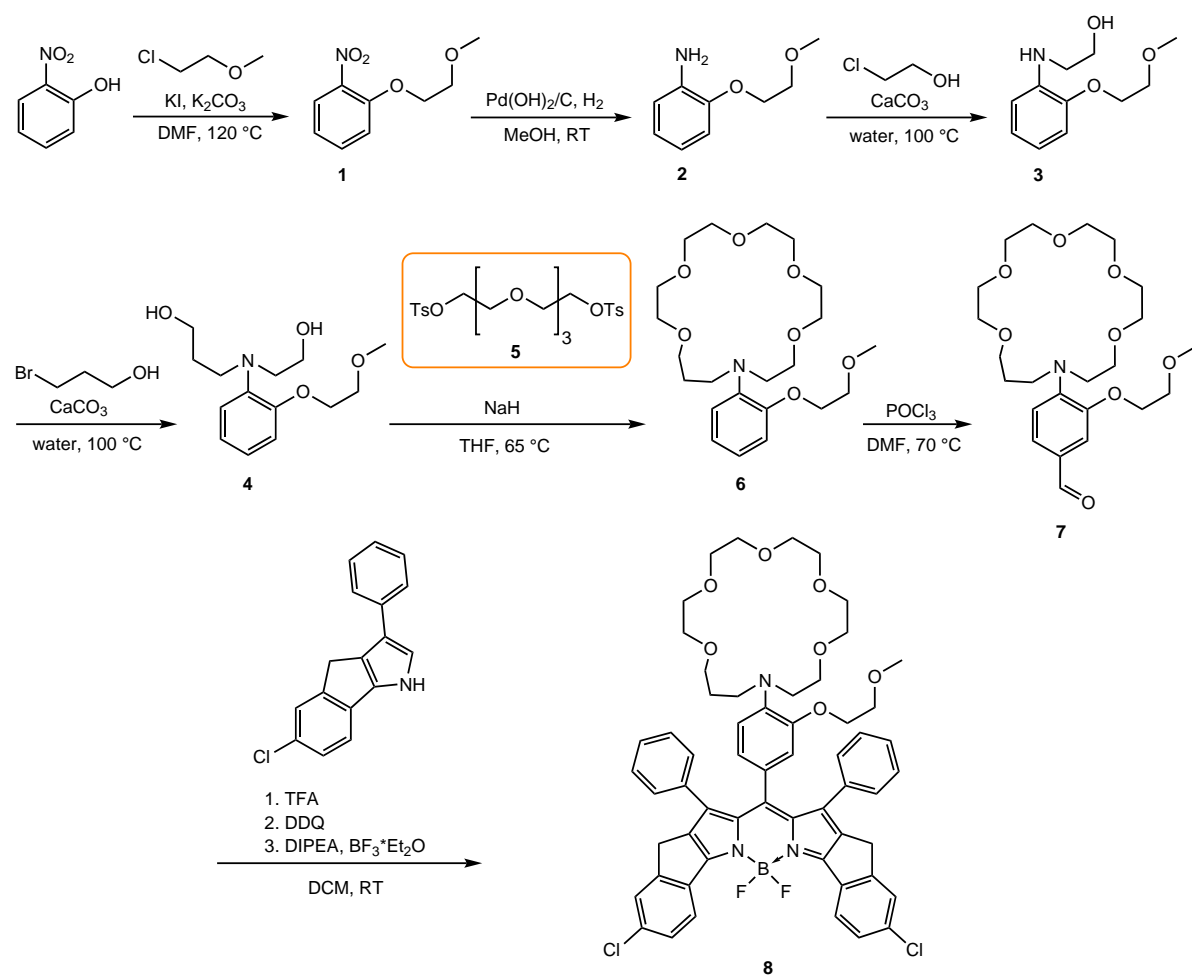
**Figure 5.20:**  
D1 and D1/PHPMA (1/3) tested polymer matrix

The polymer cocktail for this measurement was again 10 wt.% and consisted of one part hydrogel D1 and three parts PHPMA. In figure 5.20 a comparison of the calibration curves of hydrogel D1 with, and without PHPMA is shown. Without the PHPMA a  $F/F_0$  value of 3.0 was obtained and with PHPMA an even higher value of 3.5 was measured. This result is of high interest and will be investigated in the future.

## 5.4 Part 3: Synthesis of Crown Ether and Fluoroionophore

This section deals with the synthesis of a new receptor. This receptor has an additional  $\text{CH}_2$ -group in its ring and therefore, the inner cavity size is increased. This should be beneficial for the complexation of the ammonium ion and therefore, increase the sensitivity of the ammonia sensor. The detailed reaction parameters and conditions for the whole synthesis are explained in section 4.3 on page 32.

## 5.4.1 Synthesis Overview



**Figure 5.21:**  
Synthesis - Overview

### 5.4.2 Crown Ether Synthesis

The synthesis of 1-(2-methoxyethoxy)-2-nitrobenzene (**1**) was performed as described in literature with a yield of 99%. [33]

2-(2-Methoxyethoxy)-aniline (**2**) was synthesized via a Parr Hydrogenation Apparatus. The great advantages of such an apparatus are the short reaction time due to the H<sub>2</sub>-pressure and that a big amount of reagent can be hydrogenated, in this case 10 g, resulting in a 99% consumption.

Compounds **3** and **4** were synthesized according to the literature yielding roughly 52%. [34]

The crown ether (**6**) was successfully synthesized according to the <sup>1</sup>H-NMR spectra which is shown in figure 10.7 on page 73. We are currently awaiting the MALDI-HR-MS analysis. The yield of the crown ether was 63%.

### 5.4.3 Crown Aldehyde Synthesis

Compound **7** was produced via a Vilsmeier-Haack reaction. According to the <sup>1</sup>H-NMR spectra which is shown in figure 10.7 on page 73 the aldehyde compound was obtained to roughly 60%. The spectra shows the presence of the crown with and without the aldehyde. For this compound we are awaiting the MALDI-HR-MS analysis as well.

### 5.4.4 Fluoroionophore Synthesis

The synthesis of the fluoroionophore **8** was performed two times, but unfortunately it was not possible to obtain the right compound.

The crown aldehyde was dissolved in dry DMF in a flame dried and argon flushed Schlenk flask and the corresponding pyrrole was added. One drop of TFA was added and the reaction mixture was stirred under absence of light until TLC indicated a satisfying consumption.

DDQ was added resulting in a dark green color. Then DIPEA was added, which resulted in a dark red color and after addition of BF<sub>3</sub>·Et<sub>2</sub>O the color turned dark green again. After the workup the product was purified two times via column chromatography but none of the separated compounds had shown the right spectral properties.

It seems that the complexation reaction was not successful. However, further investigations were not performed and the synthesis of the compound is still under progress in the working group.





---

## 6 Conclusion and Outlook

In this thesis new optical ammonia sensors were developed. They are based on the complexation of an ammonium ion in a fluoroionophore, which is immobilized in a polymer matrix. First, hydrophobic polymers were tested. However, as the system is based on the PET effect which is highly depending on the polarity of its environment, it was not possible to obtain a suitable sensing material using this matrix. Additionally, hydrophilic matrices were used.

As hydrophilic polymer a polyurethane hydrogel D1 was used. These hydrogels are commonly used for pH or ion sensing and show a good response to ammonia. The sensor design was based on a red emissive fluoroionophore indicator dye which was immobilized in a polymer matrix. Upon this layer a teflon membrane was attached as protective layer. The sensor has fast response and recovery times, is fully reversible and no hysteresis drift is obtained. It is also stable against pH changes and shows no response to trimethylamine and dimethylamine, which is very important for environmental or biotechnological applications.

To improve the sensor, it was intended to synthesize a new receptor, which is believed to have an optimized binding stability to ammonium ions. However, a final fluoroionophore is not synthesized until now, but is under further investigation.

Another possibility for the improvement of the sensor system could be a modification of the BODIPY system via adding electron-withdrawing substituents for example halogens, which results in a decreased  $pK_a$  value of the receptor. Therefore it could be possible to use a lower pH value for the internal buffer.



---

## 7 References

1. West, S. J., Ozawa, S., Seiler, K., Tan, S. S. S. & Simon, W. Selective ionophore-based optical sensors for ammonia measurement in air. *Analytical Chemistry* **64**, 533–540 (Mar. 1992).
2. Müller, B. J., Borisov, S. M. & Klimant, I. Red- to NIR-Emitting, BODIPY-Based, K<sup>+</sup>-Selective Fluoroionophores and Sensing Materials. *Advanced Functional Materials* **26**, 7697–7707 (Nov. 1, 2016).
3. Valeur, B. *Molecular fluorescence: principles and applications* OCLC: ocm45541665. 387 pp. (Wiley-VCH, Weinheim ; New York, 2002).
4. Lakowicz, J. R. *Principles of fluorescence spectroscopy* 3rd ed. 954 pp. (Springer, New York, 2006).
5. Gründler, P. *Chemische Sensoren: eine Einführung für Naturwissenschaftler und Ingenieure ; mit 27 Tabellen* Softcover. OCLC: 820457027. 295 pp. (Springer, Berlin, 2012).
6. Eggins, B. R. *Chemical sensors and biosensors* 273 pp. (J. Wiley, Chichester ; Hoboken, NJ, 2002).
7. Pretsch, E. The new wave of ion-selective electrodes. *TrAC. Trends in analytical chemistry* **26**, 46–51 (2007).
8. Mistlberger, G., Crespo, G. A. & Bakker, E. Ionophore-Based Optical Sensors. *Annual Review of Analytical Chemistry* **7**, 483–512 (2014).
9. Panchenko, P. A., Fedorov, Y. V., Fedorova, O. A. & Jonusauskas, G. Comparative analysis of the PET and ICT sensor properties of 1,8-naphthalimides containing aza-15-crown-5 ether moiety. *Dyes and Pigments* **98**, 347–357 (Sept. 2013).
10. Valeur, B. & Leray, I. Design principles of fluorescent molecular sensors for cation recognition. *Coordination Chemistry Reviews* **205**, 3–40 (Aug. 1, 2000).
11. C. Hamilton, G. R., K. Sahoo, S., Kamila, S., Singh, N., Kaur, N., W. Hyland, B. & F. Callan, J. Optical probes for the detection of protons, and alkali and alkaline earth metal cations. *Chemical Society Reviews* **44**, 4415–4432 (2015).
12. Treibs, A. & Kreuzer, F.-H. Difluorboryl-Komplexe von Di- und Tripyrrylmethenen. *Justus Liebigs Annalen der Chemie* **718**, 208–223 (Dec. 13, 1968).
13. Loudet, A. & Burgess, K. BODIPY Dyes and Their Derivatives: Syntheses and Spectroscopic Properties. *Chemical Reviews* **107**, 4891–4932 (Nov. 1, 2007).

14. Timmer, B., Olthuis, W. & Berg, A. v. d. Ammonia sensors and their applications—a review. *Sensors and Actuators B: Chemical* **107**, 666–677 (June 29, 2005).
15. Behera, S. N., Sharma, M., Aneja, V. P. & Balasubramanian, R. Ammonia in the atmosphere: a review on emission sources, atmospheric chemistry and deposition on terrestrial bodies. *Environmental Science and Pollution Research* **20**, 8092–8131 (Nov. 1, 2013).
16. Krupa, S. V. Effects of atmospheric ammonia (NH<sub>3</sub>) on terrestrial vegetation: a review. *Environmental Pollution* **124**, 179–221 (July 1, 2003).
17. Wallin, M., Karlsson, C.-J., Skoglundh, M. & Palmqvist, A. Selective catalytic reduction of NO<sub>x</sub> with NH<sub>3</sub> over zeolite H-ZSM-5: influence of transient ammonia supply. *Journal of Catalysis* **218**, 354–364 (Sept. 10, 2003).
18. Durbin, T. D., Wilson, R. D., Norbeck, J. M., Miller, J. W., Huai, T. & Rhee, S. H. Estimates of the emission rates of ammonia from light-duty vehicles using standard chassis dynamometer test cycles. *Atmospheric Environment* **36**, 1475–1482 (Mar. 1, 2002).
19. Mount, G. H., Rumburg, B., Havig, J., Lamb, B., Westberg, H., Yonge, D., Johnson, K. & Kincaid, R. Measurement of atmospheric ammonia at a dairy using differential optical absorption spectroscopy in the mid-ultraviolet. *Atmospheric Environment* **36**, 1799–1810 (Apr. 1, 2002).
20. Fernández-Seara, J., Sieres, J. & Vázquez, M. Distillation column configurations in ammonia–water absorption refrigeration systems. *International Journal of Refrigeration* **26**, 28–34 (Jan. 1, 2003).
21. Kearney, D. J., Hubbard, T. & Putnam, D. Breath Ammonia Measurement in Helicobacter pylori Infection. *Digestive Diseases and Sciences* **47**, 2523–2530 (Nov. 1, 2002).
22. Ament, W., Huizenga, J. R., Kort, E., Mark, T. W. v. d., Grevink, R. G. & Verkerke, G. J. Respiratory Ammonia Output and Blood Ammonia Concentration During Incremental Exercise. *International Journal of Sports Medicine* **20**, 71–77 (Feb. 1999).
23. Barsan, N. & Weimar, U. Conduction Model of Metal Oxide Gas Sensors. *Journal of Electroceramics* **7**, 143–167 (Dec. 1, 2001).
24. Tomchenko, A. A., Harmer, G. P., Marquis, B. T. & Allen, J. W. Semiconducting metal oxide sensor array for the selective detection of combustion gases. *Sensors and Actuators B: Chemical. Proceedings of the Ninth International Meeting on Chemical Sensors* **93**, 126–134 (Aug. 1, 2003).
25. Xu, C. N., Miura, N., Ishida, Y., Matsuda, K. & Yamazoe, N. Selective detection of NH<sub>3</sub> over NO in combustion exhausts by using Au and MoO<sub>3</sub> doubly promoted WO<sub>3</sub> element. *Sensors and Actuators B: Chemical* **65**, 163–165 (June 30, 2000).
26. Winquist, F., Spetz, A., Lundström, I. & Danielsson, B. Determination of ammonia in air and aqueous samples with a gas-sensitive semiconductor capacitor. *Analytica Chimica Acta* **164**, 127–138 (Jan. 1, 1984).

- 
27. Lähdesmäki, I., Lewenstam, A. & Ivaska, A. A polypyrrole-based amperometric ammonia sensor. *Talanta* **43**, 125–134 (Jan. 1, 1996).
  28. Kukla, A. L., Shirshov, Y. M. & Piletsky, S. A. Ammonia sensors based on sensitive polyaniline films. *Sensors and Actuators B: Chemical* **37**, 135–140 (Dec. 1, 1996).
  29. Searle, P. L. The berthelot or indophenol reaction and its use in the analytical chemistry of nitrogen. A review. *Analyst* **109**, 549–568 (Jan. 1, 1984).
  30. Borisov, S. M., Waldhier, M. C., Klimant, I. & Wolfbeis, O. S. Optical Carbon Dioxide Sensors Based on Silicone-Encapsulated Room-Temperature Ionic Liquids. *Chemistry of Materials* **19**, 6187–6194 (Dec. 1, 2007).
  31. He, H., Mortellaro, M. A., Leiner, M. J. P., Fraatz, R. J. & Tusa, J. K. A Fluorescent Sensor with High Selectivity and Sensitivity for Potassium in Water. *Journal of the American Chemical Society* **125**, 1468–1469 (Feb. 1, 2003).
  32. Rappitsch, T. *Optical Ion Sensors - Development of New Indicators for K<sup>+</sup> and Na<sup>+</sup> Sensing* 2017.
  33. Carpenter, R. D. & Verkman, A. S. Function-Oriented Synthesis of a Didesmethyl Triaza-cryptand Analogue for Fluorescent Potassium Ion Sensing. *European Journal of Organic Chemistry* **2011**, 1242–1248 (2011).
  34. Ast, S., Schwarze, T., Müller, H., Sukhanov, A., Michaelis, S., Wegener, J., Wolfbeis, O. S., Körzdörfer, T., Dürkop, A. & Holdt, H.-J. A Highly K<sup>+</sup>-Selective Phenylaza-[18]crown-6-Lariat-Ether-Based Fluoroionophore and Its Application in the Sensing of K<sup>+</sup> Ions with an Optical Sensor Film and in Cells. *Chemistry – A European Journal* **19**, 14911–14917 (2013).



---

## 8 List of Figures

2.1	Luminescence - Overview . . . . .	3
2.2	Franck-Condon principle of a two atom model . . . . .	5
2.3	Jablonski Diagram . . . . .	5
2.4	Types of Quenching . . . . .	7
2.5	Main classes of fluorescent sensors . . . . .	8
2.6	Setup of an ISE . . . . .	9
2.7	Working principle of an ion selective membrane . . . . .	10
2.8	Scheme of the ion-exchange process . . . . .	11
2.9	PET effect from the molecular orbital point of view: . . . . .	12
2.10	Fluorescence increase with higher ion concentrations . . . . .	12
2.11	ICT effect . . . . .	13
2.12	Examples of ionophores . . . . .	13
2.13	Basic structure of a BODIPY fluorophore . . . . .	14
2.14	Fluoroionophore . . . . .	14
2.15	Schematic representation of the nitrogencycle . . . . .	15
2.16	Mechanism of acidic/basic pH indicator . . . . .	19
3.1	Plasticizer and ionic liquid structures . . . . .	21
3.2	Polymer structures . . . . .	22
3.3	Possible hydrogel structure . . . . .	22
4.1	1-(2-methoxyethoxy)-2-nitrobenzene (1) . . . . .	32
4.2	2-(2-Methoxyethoxy)-aniline (2) . . . . .	32
4.3	(((2-Methoxyethoxy)phenyl)amino)-ethanol (3) . . . . .	33
4.4	3-((2-Hydroxyethyl)(2-(2-methoxyethoxy)phenyl)amino)propan-1-ol (4) . . . . .	34
4.5	Tetraethylene-glycol-ditosylate (5) . . . . .	34
4.6	NH <sub>4</sub> <sup>+</sup> Crown (6) . . . . .	35
4.7	NH <sub>4</sub> <sup>+</sup> Crown Aldehyde (7) . . . . .	36
5.1	Fluoroionophore . . . . .	37
5.2	Sensor setup for hydrophilic matrices . . . . .	38
5.3	Optimized fluoroionophore . . . . .	38
5.4	Solvent testing . . . . .	39
5.5	Polymer testing . . . . .	40

5.6	Polymer testing . . . . .	41
5.7	Plasticizer testing . . . . .	42
5.8	Ionic liquid testing . . . . .	42
5.9	Ammonium ocanoate with TEP and TBP . . . . .	44
5.10	10 wt.% Morpholinopolymer knivecoated on PET foil . . . . .	45
5.11	75 wt.% PEG knivecoated on PET foil . . . . .	46
5.12	50 wt.% PEG 3400 knivecoated on PET foil . . . . .	46
5.13	Influence of the internal buffer capacity . . . . .	47
5.14	Influence of internal pH value . . . . .	48
5.15	Emission and kinetic spectra with internal buffer 1000 mM and pH 6.0. . . . .	49
5.16	Response and recovery times of sensor system to ammonia and buffer solution .	49
5.17	pH dependency of the sensor system . . . . .	50
5.18	Cross sensitivity to other amines and potassium . . . . .	51
5.19	TAC-BODIPY fluoroionophore . . . . .	52
5.20	D1/PHPMA polymer matrix . . . . .	53
5.21	Synthesis - Overview . . . . .	54
10.1	<sup>1</sup> H-NMR spectrum of compound <b>1</b> . . . . .	67
10.2	<sup>1</sup> H-NMR spectrum of compound <b>2</b> . . . . .	68
10.3	<sup>1</sup> H-NMR spectrum of compound <b>3</b> . . . . .	69
10.4	<sup>1</sup> H-NMR spectrum of compound <b>4</b> . . . . .	70
10.5	<sup>1</sup> H-NMR spectrum of compound <b>5</b> . . . . .	71
10.6	<sup>1</sup> H-NMR spectrum of compound <b>6</b> . . . . .	72
10.7	<sup>1</sup> H-NMR spectrum of compound <b>7</b> . . . . .	73



---

## 9 List of Tables

3.1	List of Plasticizers . . . . .	21
3.2	List of Polymers . . . . .	22
3.3	List of Chemicals . . . . .	23
3.4	List of Solvents . . . . .	24
4.1	Ammonium chloride amounts for 50 mL buffer solution . . . . .	27
4.2	Composition of polymer/DOS cocktails . . . . .	28
4.3	Composition of polymer/TBP cocktails . . . . .	28
4.4	Composition of polymer cocktails used for polymer studies . . . . .	29
4.5	Amine amounts for 250 mL . . . . .	30
4.6	pH Buffers . . . . .	31
5.1	Solubility of salts in plasticizers and obtained spectra . . . . .	43
10.1	Abbreviations . . . . .	74



# 10 Appendix

## 10.1 $^1\text{H-NMR}$ Spectra

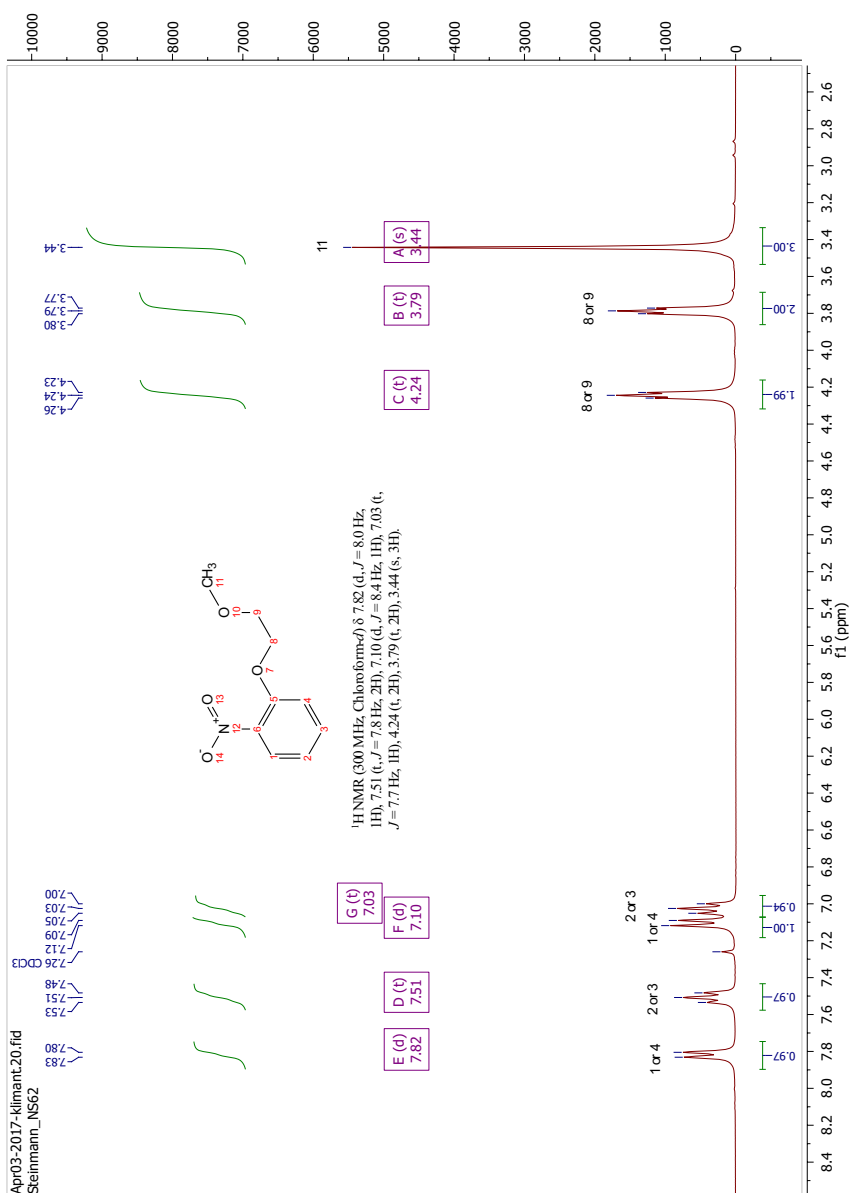
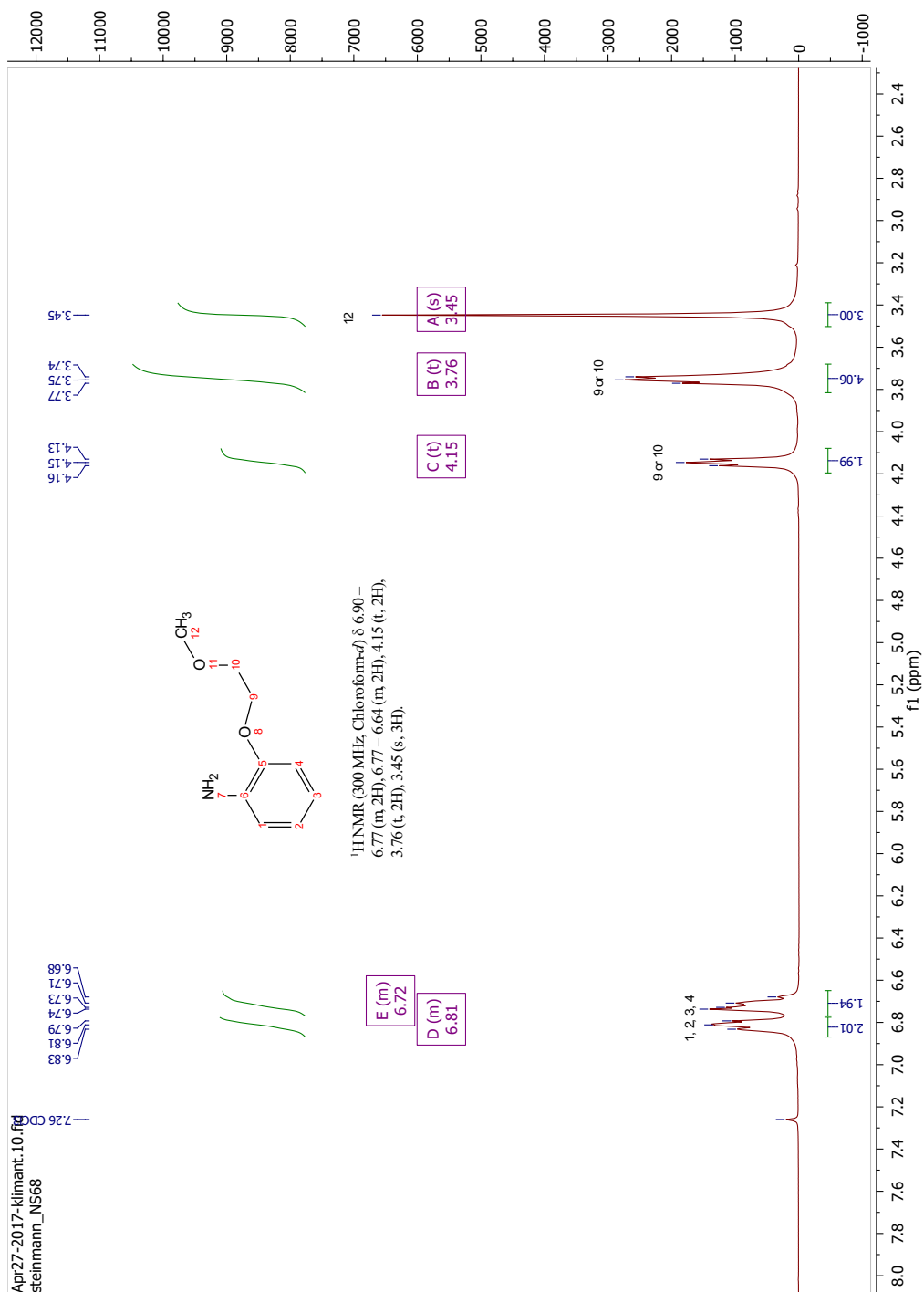
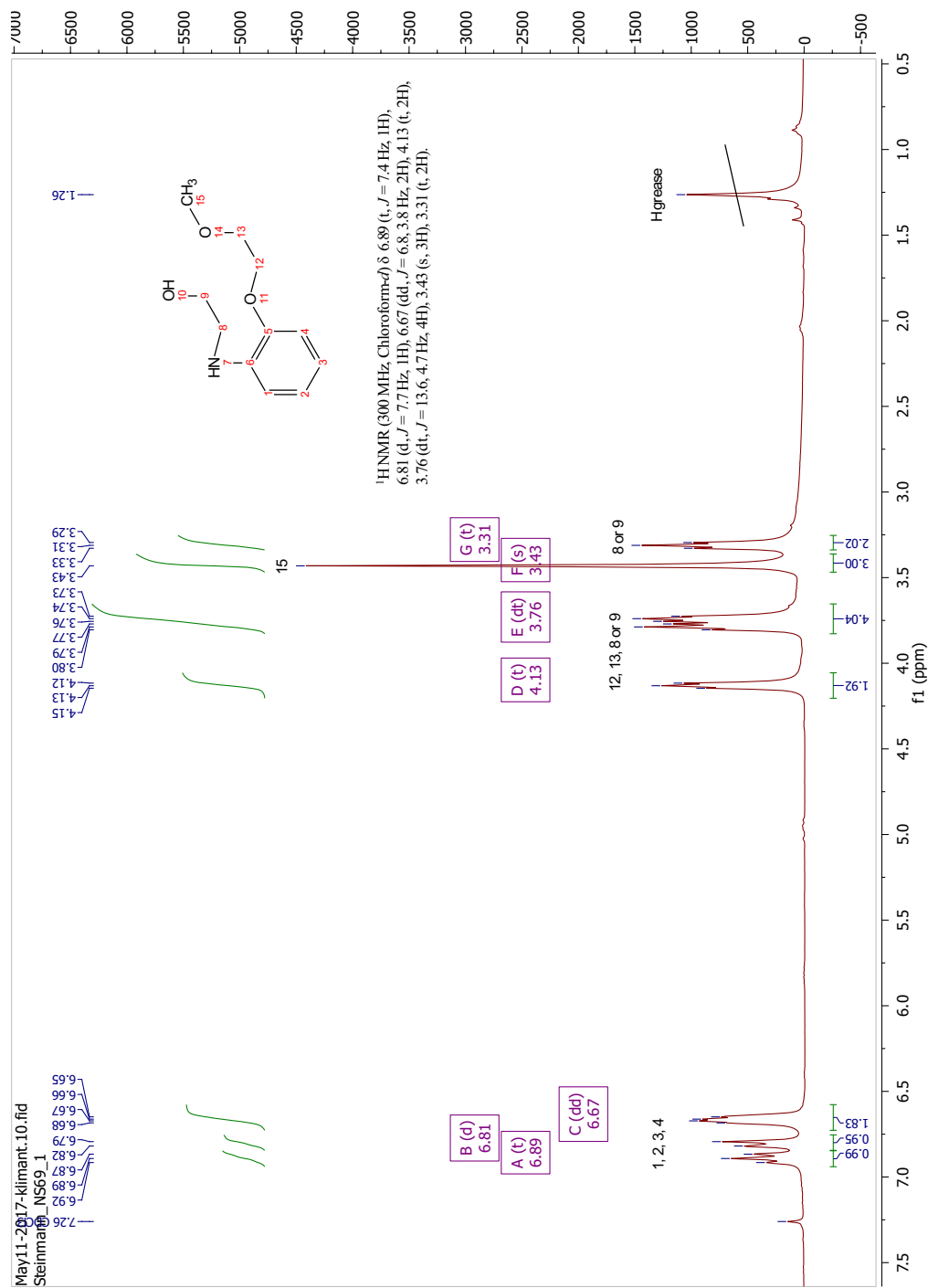
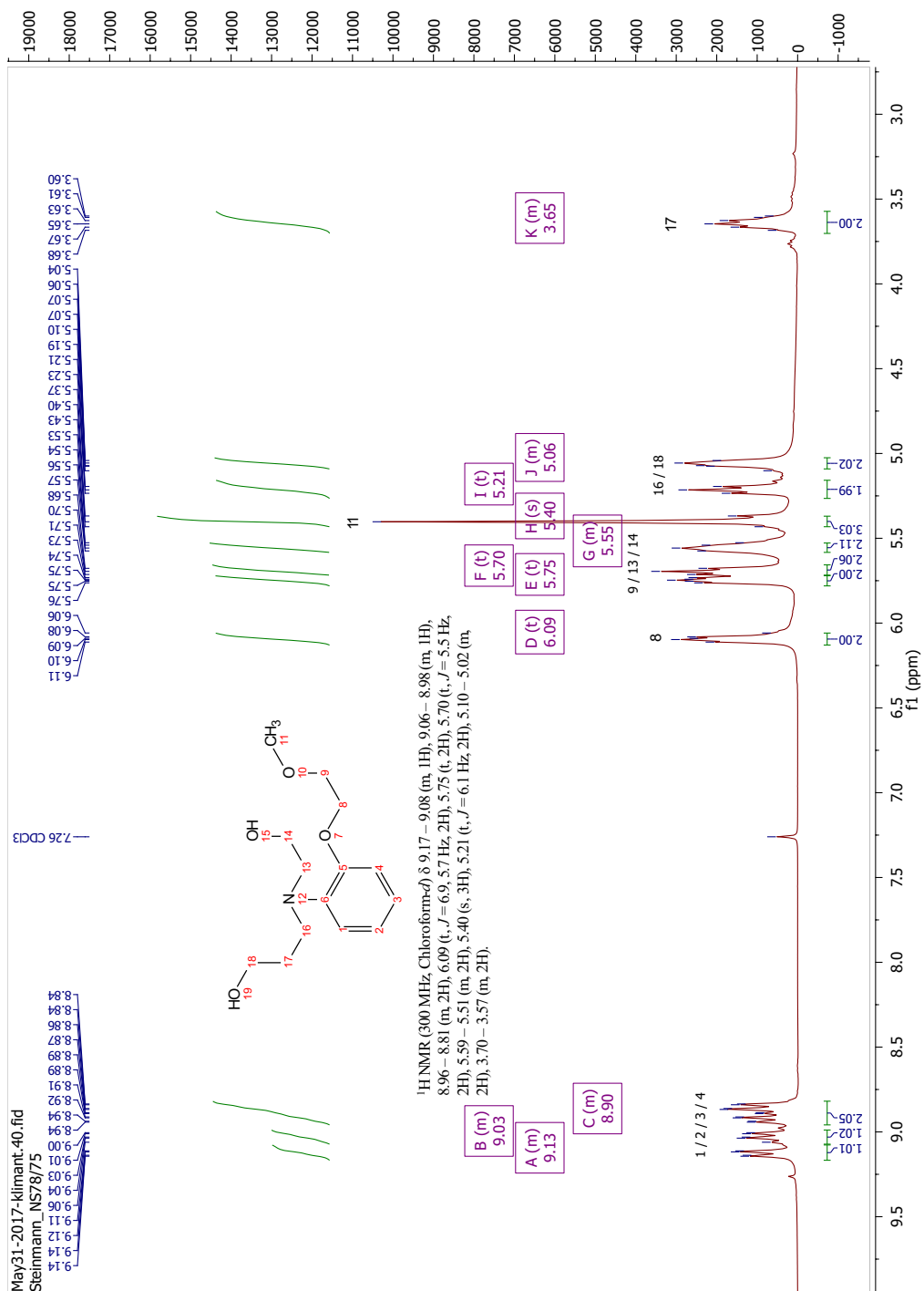


Figure 10.1:  $^1\text{H-NMR}$  spectrum of compound 1

**Figure 10.2:** <sup>1</sup>H-NMR spectrum of compound **2**



**Figure 10.3:** <sup>1</sup>H-NMR spectrum of compound **3**

Figure 10.4:  $^1\text{H}$ -NMR spectrum of compound 4

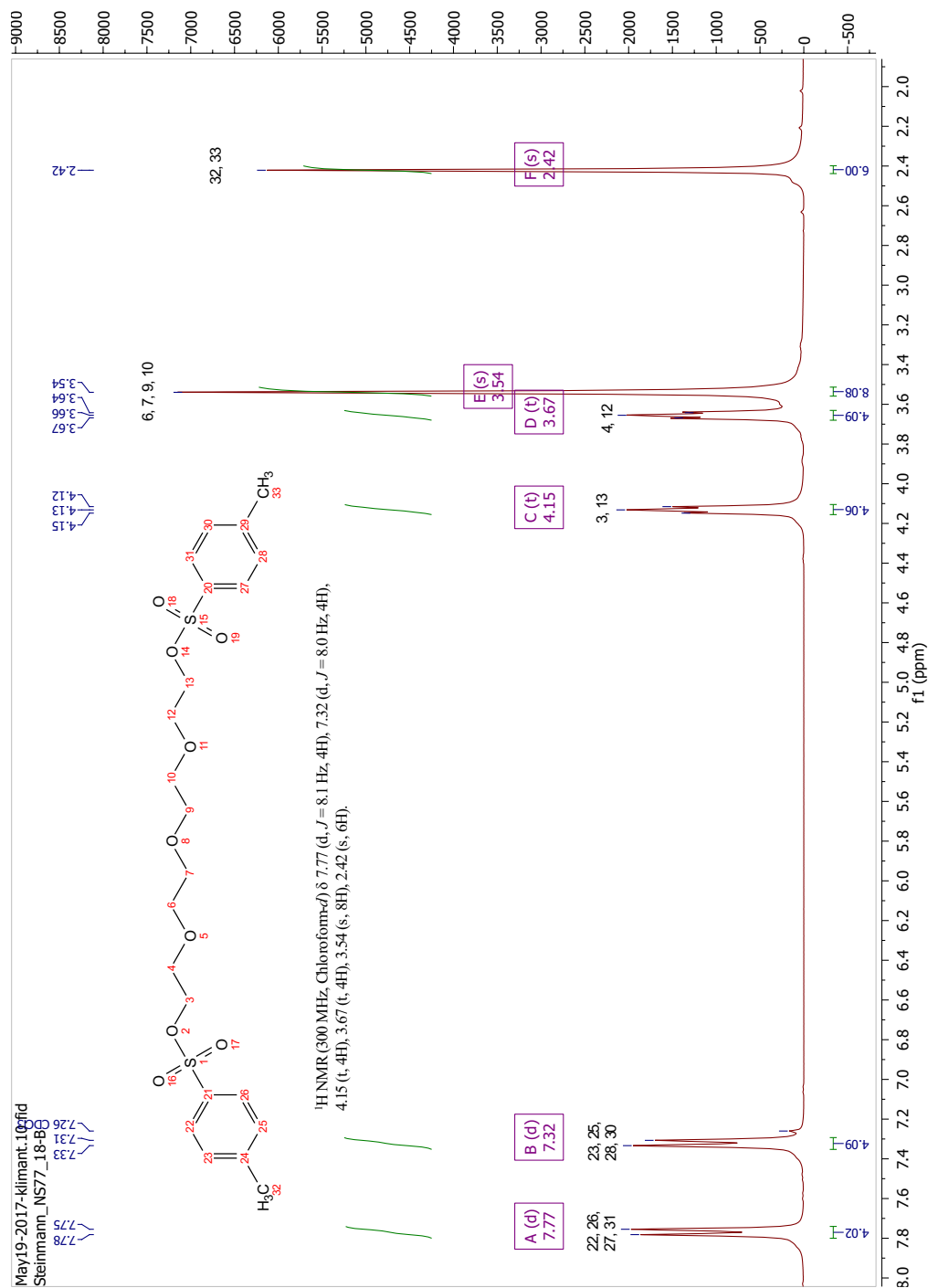
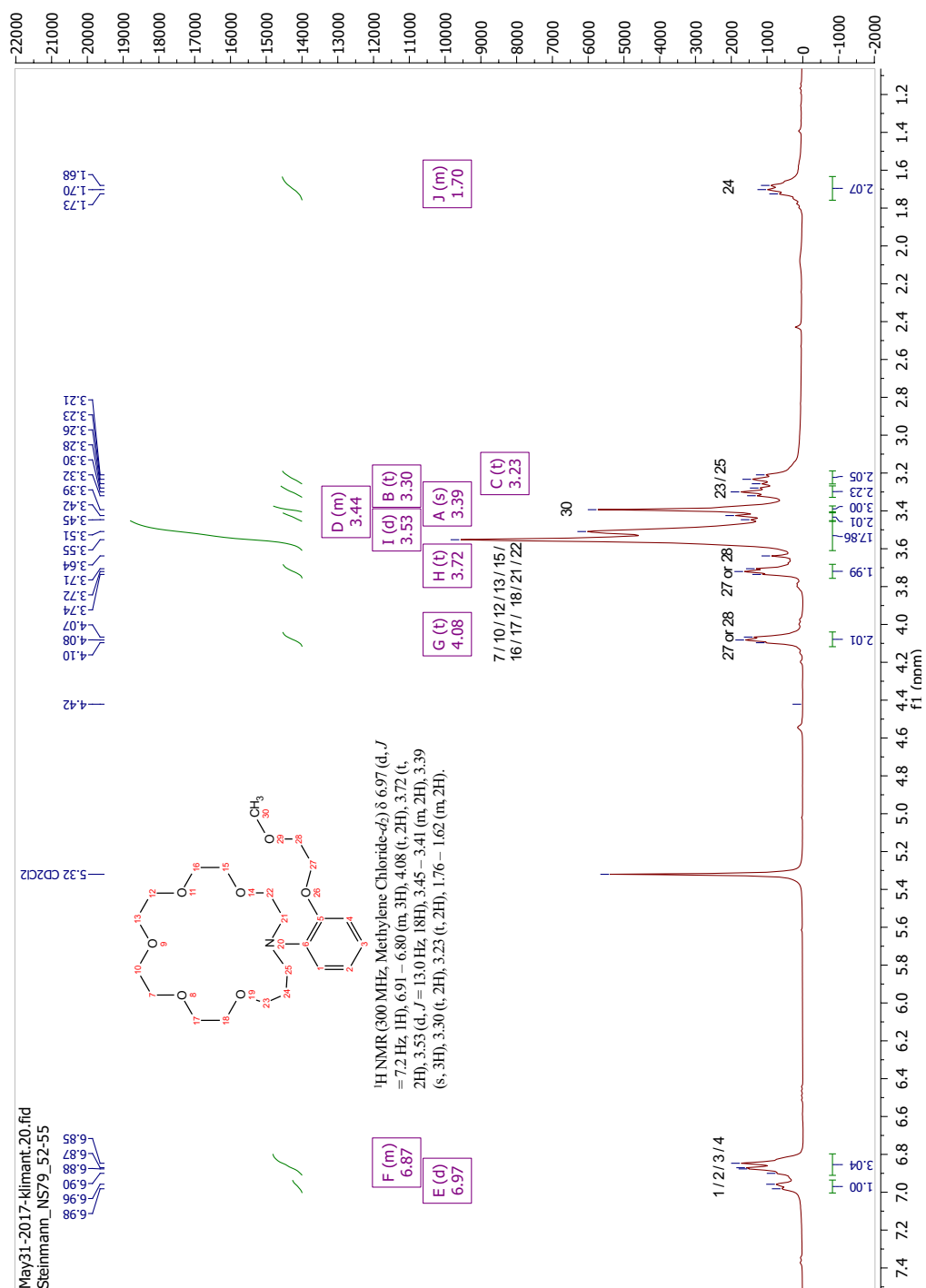
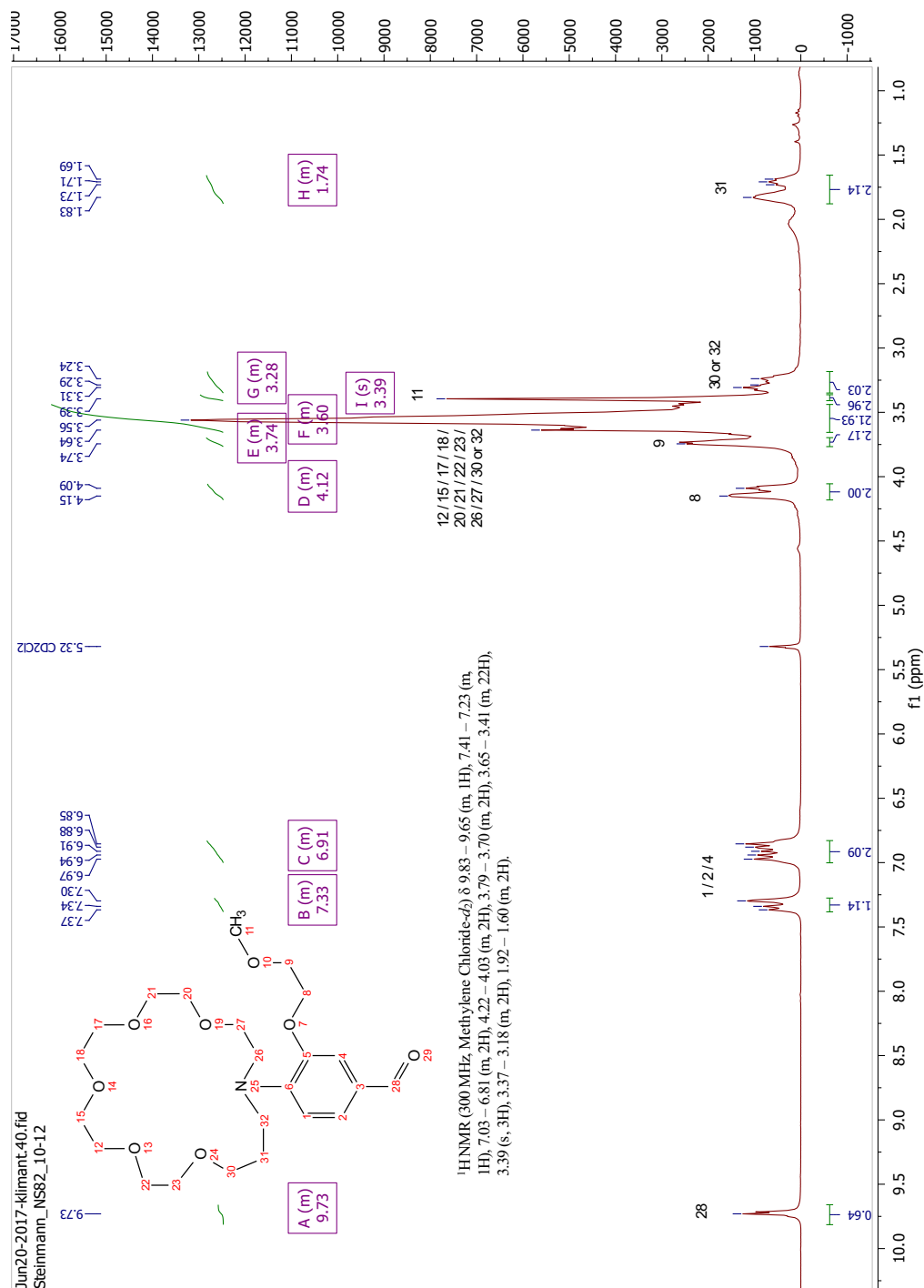


Figure 10.5:  $^1\text{H-NMR}$  spectrum of compound 5

Figure 10.6: <sup>1</sup>H-NMR spectrum of compound 6



Figure 10.7: <sup>1</sup>H-NMR spectrum of compound 7

## 10.2 Abbreviations

**Table 10.1:** Abbreviations

Å	Angstrom
BODYPI	Boron-dipyrromethene
CAM	Cer Ammonium Molybdate
CAS	Chemical Abstracts Service
CEF	Chelation/Complexation Enhancement of Fluorescence
CEQ	Chelation/Complexation Enhancement of Quenching
conc.	concentrated
dest.	distilled
DVM	Digital voltmeter
FBOS	Fluoroionophore Based Optical Sensors
FI	Fluoroionophore
GC-MS	Gas Chromatography - Mass Spectrometry
HOMO	Highest occupied molecular orbital
IBOS	Ionophore Based Optical Sensors
IC	Internal Conversion
ICT	Intramolecular Charge Transfer
IL	Ionic liquids
ISC	Inter System Crossing
ISE	Ion selective electrode
LUMO	lowest unoccupied molecular orbital
M	Molar
PET effect	Photo induced electron transfer
PET foil	Polyethylene terephthalate
ppb	parts per billion
ppm	parts per million
rev.	reverse
rt.	room temperature
s	seconds
sat.	saturated
TLC	Thin layer chromatography
UV	Ultraviolet
wt.%	weight percent
NMR	Nuclear Magnetic Resonance Spectroscopy
d	duplet
dd	doublet of doublets
Hz	Hertz
m	multiplet
s	singlet
t	triplet